Whole Number 279, ISSN 0429-8284

FUJI ELECTRIC REVIEW

2022 Vol.68 No. 4

Power Semiconductors Contributing to Mobility and Energy Management

Fuji Electric

Innovating Energy Technology

FUJI ELECTRIC
REVIEW

2022
Vol.68 No. 4

Power Semiconductors Contributing to Mobility and Energy Management

As the global trend of striving to achieve carbon neutrality is accelerating, which is aimed at solving climate change, Fuji Electric has established its Environmental Vision 2050 to determine the direction of the Company's long term environmental activities. It has set the Fiscal 2030 Goals toward reaching the Vision, one of which is the "contributions to CO_2 emissions reductions in society through our products." Among the essential factors to achieve the goal are mobility electrification and stable, efficient use of energy through the efficiency enhancement of power electronics equipment, and semiconductors from Fuji Electric play an important role in such improvements. This special issue presents the latest technologies and products in Fuji Electrics' power semiconductors.

Cover Photo:

(1) 2nd-Generation 1,700-V All-SiC Modules for industrial applications
(2) "M677" IGBT module for xEVs
(3) "P639" new compact 7th-generation IGBT-IPMs

The archives from the first issue, including articles in this issue, are available from the URLs below.

FUJI ELECTRIC REVIEW (English)
https://www.fujielectric.com/company/tech/contents3.html

FUJI ELECTRIC JOURNAL (Japanese)
https://www.fujielectric.co.jp/about/company/contents_02_03.html
FUJI ELECTRIC JOURNAL (Chinese)
http://www.fujielectric.com.cn/jtkw.html

FUJI ELECTRIC REVIEW vol.68 no.4 2022
date of issue: March 30, 2023

editor-in-chief and publisher **NAKAYAMA, Kazuya**
Corporate R&D Headquarters
Fuji Electric Co., Ltd.
Gate City Ohsaki, East Tower,
11-2, Osaki 1-chome, Shinagawa-ku,
Tokyo 141-0032, Japan

editorial office Fuji Electric Journal Editorial Office
c/o Fuji Office & Life Service Co., Ltd.
1, Fujimachi, Hino-shi, Tokyo 191-8502,
Japan

The original Japanese version of this journal is "FUJI ELECTRIC JOURNAL" vol.95 no.4

Contents

Preface

Power Semiconductor Devices — Driving Technology for Power Conversion Systems

LORENZ, Leo*

Power Electronics is the key technology to control the flow of electrical energy along the whole chain from generation, transmission and distribution up to various types of consumers, and to do so with great precision, extremely fast dynamic control, high efficiency, and high-power density on all power conversion stages. Furthermore, this technology is an enabler for the grid integration of renewable energy sources and E-Mobility and provide significant contributions to the key issues of improved energy efficiency, reduced consumption of materials as well as the sustainable energy supply based on renewables.

Sustainability and Global Warming

Power electronics is a cross-sectional and ubiquitous field as it covers many disciplines including material science, semiconductor physics, assembly and interconnection technologies, circuit topologies and control, in all applications dealing with electric energy. Today we know that changes in all energy sectors are needed, and that renewables-based electrification is the major step towards greenhouse gas reduction and climate change mitigation.

Mobility is key for global growth and societal wealth. As such, mobility is undergoing a transformation from fossil fuel mobility to sustainable and environmentally friendly electric mobility. In addition, electrification allows the rise of new mobility concepts such as drones and high-speed transportation like the hyperloop concept. In general power electronics for electric vehicles have progressed well with transitioning from Silicon based switching devices to SiC and GaN switching devices. Integration of the electric motor and the inverter is seen as a key development to achieve better integration and standardization. Challenges here are new active or hybrid EMC filter technologies to reduce size, weight, and costs.

Trucks and busses share the same roads as cars, but energy and power demands are higher, and the operation time is much longer. Power electronics is therefore designed to deal with higher lifetime requirements.

From all transportation systems, railway is the most experienced electrification so far. Trains and infrastructure are expected to last decades and as such power electronics must offer high reliability and long lifetime. The need for very high-speed trains is growing resulting in the development and implementation of MAGLEV trains and Hyperloop vehicles.

Emissions and noise from aircrafts must be reduced by 2040 and electrification will undoubtedly help in achieving these targets. In these application, semiconductors like SiC and GaN are needed and for the future even ultra-wide bandgap semiconductors (UWBG) will give an additional benefit.

Generally speaking, a lot of innovation towards smart converters using benefits from I 4.0 and AI will dominate power electronics in all fields of mobility and energy supply application. Sustainability is getting more in focus for all developments in the future.

Power semiconductor devices

The performance of active and passive power devices has always been a limiting but enabling factor for power electronics.

Silicon (Si) devices have been the workhorses of power electronics and will remain for the next decades. The low voltage MOSFET, the super junction MOSFET, the IGBT and thyristor-based devices have reached a level of maturity that ground-breaking innovations are not to be expected.

Two decades ago, the first silicon carbide (SiC) Schottky diode became commercially available, and one decade ago, the first SiC MOSFETs appeared on the market. In the meantime, SiC devices have reached a considerable market share and made the step out of the high-end niche into the mainstream, with the e-mobility and renewable energy technologies. Today the voltage range is covering from 650 V up to 6.5 kV and further development like the super junction MOSFET and the FinFET are attracting more and more attention.

Lateral gallium nitride (GaN) devices with voltage ratings up to 650 V are now established. There is currently a strong focus for consumer electronics but also for power supplies in ICT and data centres. All these applications take benefit from the low parasitic capacitances and the low gate charge. GaN-based converter

* Dr. Engineering, President ECPE (European Center for Power Electronics)
Technology Advisor to Industry and Government, Munich, Germany

circuits can operate at higher switching frequencies with still high efficiency and their volume and weight can be reduced significantly. Monolithic integration is an important advantage in lateral GaN technology. Vertical GaN transistors are recently considered for voltage ratings > 1,000 V and for higher current capabilities. The next step will be ultra-wide bandgap semiconductors (UWBG) made of Ga_2O_3, AlGaN, AlN or diamond crystals.

Power Electronics capability in Japan

Historically, Japan has a strong position in power electronics, on the technology side with power devices and on the application side with industry, renewable energy technologies and traction drives.

Japan industry is covering the whole value-added chain starting with materials, substrates, wafers, power devices, and converters covering a variety of applications.

From the very beginning of Power Electronics Fuji Electric is playing a key role, and in many cases, creates trend setting technologies. This issue provides an excellent example of the current technology available towards the future trends.

Power Semiconductors Contributing to Mobility and Energy Management

ONISHI, Yasuhiko* MIYASAKA, Tadashi* IKAWA, Osamu*

1. Introduction

Global efforts toward achieving carbon neutrality by reducing carbon emissions are accelerating, and Japan and other countries around the world have established specific goals to reduce greenhouse emissions. Having included in our corporate philosophy our intentions to "contribute to prosperity," "encourage creativity," and "seek harmony with the environment," Fuji Electric has established the "Environmental Vision 2050," which aims to realize a "decarbonized society," "recycling-oriented society," and "a society that is in harmony with nature" through the spread and expansion of innovative clean energy technologies and energy-saving products, with our role in the realization of a sustainable society through energy and environment businesses as a pillar of our management policies.

In particular, the key to the realization of a decarbonized society is the expansion of vehicle electrification and the efficient use of electrical power, and power electronic equipment is indispensable in achieving these goals. As key devices for power electronic equipment, power semiconductors are becoming increasingly promising.

2. Fuji Electric's Power Semiconductors

Fuji Electric develops a wide range of power semiconductors to address market demand. Figure 1 shows examples of the applications of Fuji Electric's power semiconductors.

2.1 Automotive field

Figure 2 shows the expected global sales for passenger vehicles by power source. As indicated by this chart, sales of electric motor vehicles are expected to continue growing. Fuji Electric has been developing and expanding the mass-production of automotive insulated gate bipolar transistor (IGBT)*1 modules for motor control, as well as power semiconductor products for the power conversion control of chargers and DC power supplies.

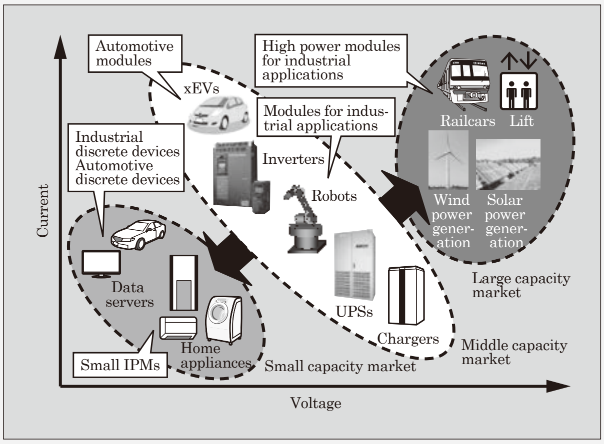

Fig.1 Examples of the application of Fuji Electric power semiconductors

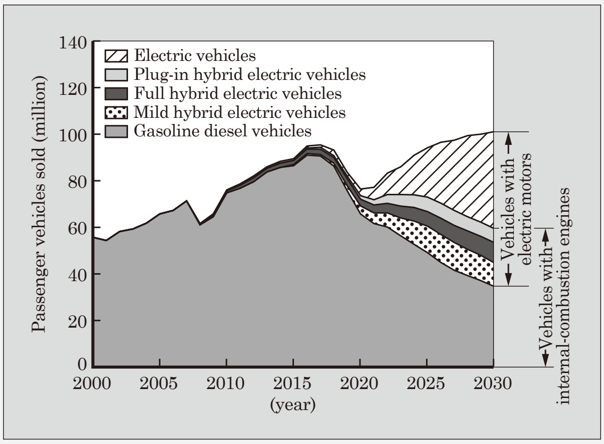

Fig.2 Estimated sales of passenger vehicles by power source (Prepared by Fuji Electric)

However, internal combustion engines are expected to remain in use as a component of hybrid electric vehicles and others with a focus on environmental performance. For such applications, Fuji Electric develops and releases automotive products, including intelligent power switches (IPSs) used to perform on-off control of the driving current for the hydraulic valves in engines and transmissions, the intake and exhaust systems in gasoline engines, pressure sensors used for the hydraulic pressure control of transmissions, power steering and brak-

* Semiconductors Business Group, Fuji Electric Co., Ltd.

ing mechanisms, and one-chip igniters used for ignition control of gasoline engines, and in this way, we contribute to the reduction of CO_2 emissions through efficient engine combustion and other achievements.

2.2 Industrial field

For industrial uses, Fuji Electric offers low, medium and high-power rating products.

We develop and release low-power rating products, including intelligent power modules (IPMs)*2 used for driving the motors of electrical appliances such as air conditioners. We also develop and release discrete*3 IGBTs mainly used for power conversion equipment, such as low-power rating power conditioning systems (PCSs) and uninterruptible power systems (UPSs). Furthermore, we develop and release power ICs for controlling the switching power supplies of LED lighting and other electronic equipment.

In the medium-power rating product field, we develop and mass-produce industrial IGBT modules to be used in general-purpose inverters, machine tools, servo motor control for robots, motor control for business-use air conditioners, and power conversion equipment in UPSs for data centers. In this field, the demand is expected to rise as investments are made in automation to address labor shortages and improve productivity.

In the high-power rating product field, we develop and release IGBT modules for power conversion equipment for renewable energy generation, including wind power and mega solar, and variable speed drives for motors in railcars.

In addition to these products, Fuji Electric develops and releases silicon carbide (SiC)*4 devices, which are next-generation power semiconductors with better characteristics compared with existing silicone (Si) devices, such as low loss, high breakdown voltage, and high temperature operation.

3. The State of Power Semiconductor Development

This chapter showcases Fuji Electric's latest achievements in the development of power semiconductors.

3.1 Packaging technologies that achieve high power density in IGBT modules for xEVs

Automotive IGBT modules used for controlling the driving motors of electrified vehicles (xEVs) must be made compact enough to fit in limited spaces and also require higher power density to meet the demand for higher output. As a result of efforts to develop the semiconductor devices and packaging technologies required to achieve higher power density in power modules, Fuji Electric has developed an industry-leading, ultra-compact IGBT module for xEVs, the "M677" made for 100-kW class inverters as a key component of xEV power trains (see Fig. 3).[(1),(2)] To achieve reduced size and increased output power, we have equipped the M677 with a 7th-generation reverse conducting IGBT (RC-IGBT)*5, and in order to reduce conduc-

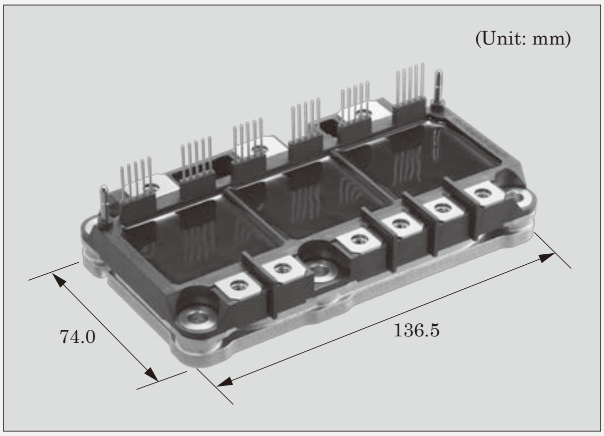

Fig. 3 "M677" IGBT module for xEVs

***1 IGBT**

IGBT is an initialism for insulated gate bipolar transistor. It is a voltage controlled device with a gate that is insulated with an oxide insulation layer, the gate structure of which is the same as that of MOSFETs. It makes use of the advantages of MOSFETs and bipolar transistors. Its bipolar functionality enables the use of conductivity modulation, and it features both high switching speed and high-voltage resistance and low on-state resistance, which are sufficient for inverter applications.

***2 IPM**

IPM is an initialism for intelligent power module. These power modules have built-in driver circuits and protection circuits in addition to power semiconductor components. In addition to reducing the burden of circuit design, the use of dedicated drive circuits maximizes the performance of the power semiconductor components.

***3 Discrete**

The word discrete is used to describe power semiconductor devices that consist of a single power semiconductor IGBT or MOSFET or a circuit called a 1 in 1, in which diodes are inserted in anti-parallel configuration. Pin layouts are determined for general purpose uses, with variations such as TO-220 and TO-3P. These devices are used to control circuits of small capacities, including PC power supplies, uninterruptible power systems, liquid crystal displays, and small motors.

***4 SiC**

SiC is a compound of silicon (Si) and carbon (C). There are a variety of SiC polymorphic crystal structures, such as 3C, 4H, and 6H, and the compound is known as a wide gap semiconductor with bandgaps of 2.2 to 3.3 eV. Due to its high electric breakdown voltage and heat conductivity, it is useful for power devices, and it is increasingly being used to produce devices that feature high breakdown voltage, low loss, and high-temperature operation.

tion loss, we reduced the Si wafer thickness and optimized the surface structure. As a measure to address the tendency for the internal temperature to rise in conjunction with the reduction of thermal capacity caused by the reduced chip volume, we use copper lead frames, which have higher heat dissipation properties than conventional aluminum wires. This results in a 40% improvement compared with the predecessor product in terms of the short-circuit failure energy that damages the chip due to thermal runaway attributable to, for example, leak current.

Moreover, we confirmed that this package is sufficiently resistant to electromigration, which has the potential to cause increases in wiring resistance and thermal resistance if the module is used in high power density or high temperature environments. (Refer to page 175, "Package Technology for achieving High Power Density in IGBT Modules for xEVs").

3.2 Line-up expansion of the 2nd-generation 1,700-V All-SiC modules

Since the power electronic equipment used in 690-V AC motor drives and railcars operate at a DC bus voltage of 900 to 1,100 V, there is demand for power semiconductors rated at 1,700 V. In addition, higher DC bus voltages are required in the renewable energy sectors, including solar and wind power generation, to improve power generation efficiency and reduce costs.[3] For use in industries in which high withstand-voltage power semiconductors are sought, Fuji Electric previously developed a 1,700-V All-SiC module equipped with a 2nd-generation SiC trench gate metal-oxide-semiconductor field-effect transistor (MOSFET)[4], and has now added a newly developed product to this line-up.

Compared with the 3-level NPC circuit configured with the predecessor 1,200-V Si-IGBT, the 2-level circuit configured with the newly developed 1,700-V All-SiC module has achieved a 69% reduction in the total loss when applied to power electronic equipment with a DC bus voltage of 1,100 V (see Fig. 4). In addition to the expected high efficiency, switching from a 3-level circuit configuration to a 2-level one can reduce the number of power semiconductor devices, which is expected to increase the reliability of power electronics equipment and reduce costs.

SiC-MOSFETs are capable of much faster switching than Si-IGBTs, but have the disadvantage of causing high surge voltages during high-speed switching due to the wiring inductance inside the

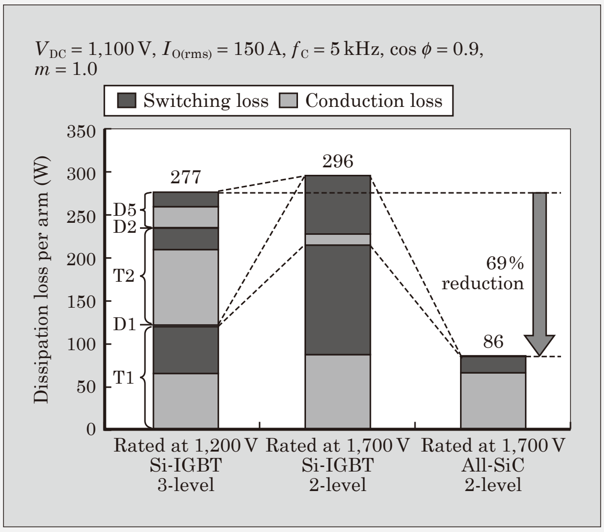

Fig.4 Loss comparison with 3-level and 2-level circuits

module. For the All-SiC module, the new product in the line-up, we have reduced the wiring inductance by 24% by changing the internal structure[4], but the Si-IGBT can be replaced with this product easily because its external shape and terminal layout are still compatible with the 7th-generation "X Series" IGBT's 2-in-1 package "M276" (Refer to page 180, "Line-Up Expansion of 2nd-generation 1,700-V All-SiC Modules").

3.3 Line-up of compact 7th-generation IGBT-IPMs with RC-IGBTs

As the adoption of factory automation and communication devices including mobile phones has become more widespread in recent years, the demand for servo systems used for industrial robots, machine tools, and other applications has increased. Space saving is a critical requirement for such devices, and to achieve this, the size of the power semiconductors used in these devices must also be reduced, the key to which is high temperature operation and low loss. In addition, they are required to be highly reliable to prevent sudden malfunctions.

IGBT-intelligent power modules (IPMs), which are IGBT modules equipped with a control IC for driving the IGBT gate as well as a protection function, have highly reliable diverse applications, such as numerical control (NC) machine tools, robots, and elevators.

To achieve low power dissipation, the 7th-generation IGBT-IPM[5]-[8], which is the newest generation of IGBT-IPMs, employs 7th-generation chip technology, in which the IGBT trench gate structure is made finer and the drift layer is made thinner

***5 RC-IGBT**

RC-IGBT is an initialism for reverse-conducting IGBT. They are components that integrate the IGBT and FWD into a single chip. The IGBT and FWD sections operate alternately, resulting in excellent heat dissipation and reducing the number of chips in the module, leading to smaller IGBT modules and higher power density.

through the use of thin wafer processing technology, as well as a new control technology for driving the IGBT gate. Furthermore, it can operate under high temperatures due to 7th-generation packaging technology, which includes high heat resistant gel and highly reliable solder. In order to meet the demand for further size reduction and high reliability, we have added products that make use of RC-IGBT chips to 7th-generation IGBT-IPM line-up. The RC-IGBT chip combines the IGBT chip and the free wheel diode (FWD)*6 chip on a single chip.

Reduction of package size is now possible with the use of the RC-IGBT, which has reduced the total chip footprint by 33% compared with the 6th-generation IGBT-IPM, which is configured with independent IGBT and FWD chips. In addition, 7th-generation chip technologies and a new control technology have reduced power dissipation by approximately 7% compared with the 6th-generation IGBT-IPM. With the reduction in chip footprint and power dissipation, the newly developed compact package "P639" has reduced the footprint of the copper base, which dissipates chip heat by 33% compared with the predecessor, and has thereby reduced the package's area by 27%. Furthermore, the ΔT_{vj} power cycling lifetime, which is a typical lifetime characteristic of power modules, has also increased through the use of the RC-IGBT. The predecessor 6th-generation IGBT-IPM has the IGBT and FWD alternately repeating heating and cooling, whereas the RC-IGBT integrates the IGBT region and the FWD region into one chip, and therefore, the temperature change ΔT_{vj} of the entire chip is smaller than that of the independent chips. Because of this, power cycling lifetime ΔT_{vj} in relation to the junction areas' wear-out failure caused by temperature changes is estimated to be approximately 10 times longer than that of the 6th-generation model during operation at an output frequency of 1 Hz.

As an example, if the predecessor "P629" used in a 60-mm width back-fin type servo amplifier is replaced by the newly developed P639, the servo amplifier's casing can be reduced in width to the order of 46.5 mm, which is a reduction of approximately 20% (see Fig. 5) (Refer to page 185, "Line-Up of Compact 7th-Generation IGBT-IPMs with RC-IGBTs").

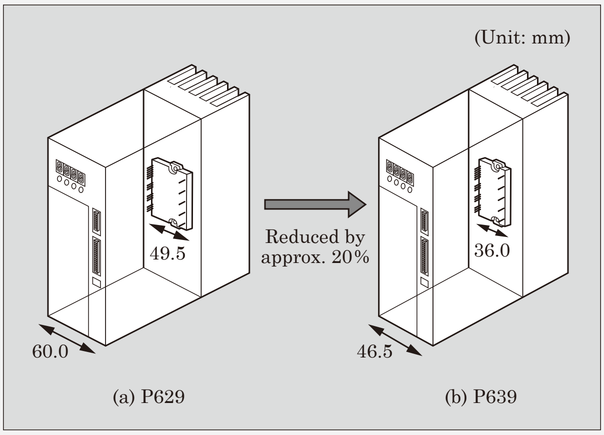

Fig.5 Schematic diagram of a back-fin type servo amplifier

3.4 3.3-kV 7th-generation "X Series" IGBT chip technology

High-speed rail vehicles emit far less CO_2 than airplanes, which achieve the same function of long-distance transport. For this reason, in recent years, the introduction of high-speed rail has been increasing not only in Japan but also around the world. Railway vehicles use IGBT modules to drive their motors. To reduce CO_2 emissions, IGBT modules require further reductions in power loss. In addition, to reduce the power consumption of high-speed trains themselves, the weight reduction of the vehicles and their on-board equipment is important and requires IGBT modules that can facilitate the size and weight reduction of the system.

Fuji Electric has developed the 3.3-kV SiC hybrid high power module (HPM), which combines the newest-generation "X Series" IGBT and a Schottky barrier diode*7 (SiC-SBD), thereby achieving significant reductions in power loss.[9]

The newly developed 3.3-kV X-Series IGBT chip (X-IGBT) has a more optimized surface structure and a thinner n^- drift layer, which, compared with the predecessor product, results in a 1.0 V reduction in collector-emitter saturation voltage $V_{CE(sat)}$ at rated current, which is an indicator of conduction loss.

Figure 6 shows the relationship between the turn-off loss E_{off} and $V_{CE(sat)}$. With the X-IGBT, $V_{CE(sat)}$, when compared at the same E_{off}, has been

***6 FWD**

FWD is an initialism for free wheeling diode. It is also called a reverse-conducting diode. This component is connected parallel to an IGBT in power conversion circuits, such as inverters, and are responsible for returning the energy stored in the inductance to the power supply side when the IGBT is turned off. P-intrinsic-N (PiN) diodes are used mainly for Si FWDs. They are bipolar diodes that also use minority carriers, and therefore, they enable the reduction of voltage drop during forward current flow, but they also cause larger reverse recovery losses.

***7 SBD**

SBD is an initialism for Schottky barrier diode. They are diodes with rectifying action that uses the Schottky barrier created by the junction of a metal and a semiconductor. Due to their excellent electric characteristics, studies on their application in FWDs for SiC-SBDs are underway. In comparison with PiN diodes that also use minority carriers, SBDs operate with majority carriers only, and have faster reverse recovery speed and lower reverse recovery loss.

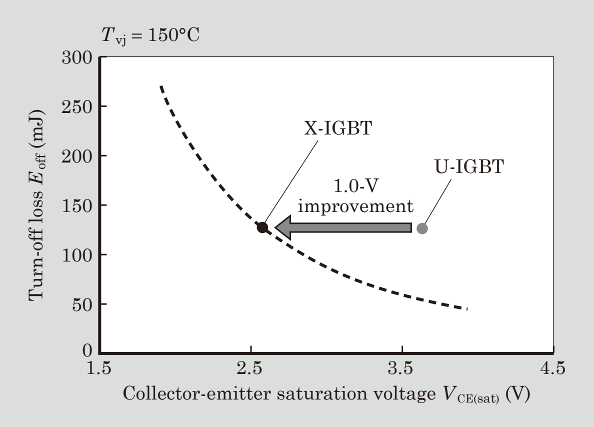

Fig.6 Relationship between the turn-off loss and the collector-emitter saturation voltage

reduced by 1.0 V compared with the predecessor product. In addition, the finer surface structure improved the control performance with gate resistance dv/dt, di/dt during turn-on, resulting in improvements in turn-on loss E_{on}.

The 3.3-kV SiC hybrid HPMs equipped with this IGBT are employed in high-speed rail vehicles that are now in commercial service, and the IGBT is contributing to reductions in power consumption of high-speed rail vehicles and the size and weight reduction of equipment (Refer to page 190, "3.3-kV 7th-Generation "X Series" IGBT Chip Technology").

3.5 "FA8C00 Series" of 7th-generation PWM power supply control ICs

Energy-saving requirements for switching power supplies used in electronics are growing stricter, and in particular, improvements in power conversion efficiency for low loads are urgently required as the use of networks expands and more systems are in constant operation. In emerging economies, slow progress in infrastructure development causes commercial power supply (AC power supply) voltage to fluctuate frequently. This causes high voltages in the AC power supply, and damages to power supply units that occur when the input voltage range of power supply units is exceeded have become a problem. Moreover, there is an urgent demand to reduce the number of components in power supplies in response to the continued need for low cost electronic equipment.

Fuji Electric has recently developed the "FA8C00 Series," which can further improve power conversion efficiency at low loads on power supply systems compared with its predecessor[10], support high AC input voltages, and reduce the number of power supply components. Table 1 shows a functional overview of the FA8C00 Series.

In order to improve power conversion efficiency at low loads, a conventional method of reducing MOSFET switching losses has been employed by performing burst operation, in which continuous switching operation and switching stoppage are repeated. To further improve power conversion efficiency in this operation, it is effective to optimize the output pulse width to match the power supply to avoid generating output pulses for driving MOSFETs with narrow widths. With the addition of a function to set the minimum output pulse width according to the power supply, the FA8C00 Series can now improve power conversion efficiency at low loads.

Table 1 "FA8C00 Series" function overview

Item	Conventional product	FA8C00 Series
Minimum output pulse width select function	Not provided	Available
Maximum applied voltage of the high AC input voltage terminal	650 V	710 V
IC output voltage clamp function	Not provided	Available (16 V)
External regulator	Required	Not required (8 parts reducible.)

In addition, we have improved the start-up device used in the internal circuit of the high voltage AC input terminal (VH terminal) for utility power connection. Increasing the rated maximum input voltage of the device to 710 V has allowed it to prevent the breakdown caused by the fluctuation of the AC power source.

On the other hand, the rated voltage of the gate terminal of MOSFETs driven by the power supply IC is 20 to 30 V, and applying a higher voltage can damage the MOSFETs. To prevent this, the previous product required an external regulator circuit to limit the VCC terminal's voltage, which is the power supply voltage of the driver circuit for driving the MOSFET, to 20 V or below. In the new series, the FA8C00, the function of clamping the output terminal's voltage inside the IC has been incorporated so that the gate voltage output from the IC is regulated at 16 V even if the VCC terminal's voltage exceeds 30 V. This improvement has eliminated the need for an external regulator circuit and facilitated the reduction of power supply parts (Refer to page 194, "'FA8C00 Series' 7th-Generation PWM Power Supply Control ICs").

3.6 Auto-zero amplifier technology for IPS

Fuji Electric has been developing and releasing IPSs[11],[12], which are current drive devices to operate the solenoid valves for controlling automotive transmission systems. The size reduction of IPSs and the integration of peripherals into one chip are measures that can reduce the size of electronic control unit (ECU) boards, thereby providing vehicles with more interior comfort. Improvements in the current detection accuracy of IPSs can improve fuel efficiency. When the IPS and the shunt resistor for current detection, which has been previously placed separately, are integrated into a single chip, the Joule heat generated by the shunt resistor causes the chip temperature to rise. The remedial suppression of this rise in chip temperature requires the shunt resistance to reduce to one-fourth of the conventional value. Although accommodating the resistance reduction while maintaining the input current-amplifier output voltage characteristics requires the increase of the differential gain of the amplifier to four times the conventional gain, this measure causes the disadvantage of increased amplifier output errors and worsened current detection accuracy. To resolve this, we have developed the auto-zero amplifier technology that self-corrects the offset voltage at specified intervals.

Figure 7 shows the evaluation results of an actual device using an auto-zero amplifier. In this evaluation, we set the gain to be 32 times, which is four times greater than the conventional amplifier, considering the need to reduce the shunt resistor's resistance to one-fourth the conventional resistance. To the amplifier input, we applied a load current of 1 A and a voltage that allows the shunt resistance to be one-fourth the conventional resistance. Under these conditions, we conducted an evaluation of current detection accuracy within the temperature range of −40 °C to +175 °C. The target value for current detection accuracy was set to be ±3.1% or lower, which is the same as 5th-generation IPSs[13]. The results showed that it met the target specification of the 5th-generation IPS despite the fact that we set the gain to be 32 times, which is four times greater than with the conventional amplifier.

This suggests that the mounting footprint of ECU boards can be expected to be reduced while preserving a current detection accuracy that is equivalent to the conventional level (Refer to page 199, "Auto-Zero Amplifier Technology for Intelligent Power Switches").

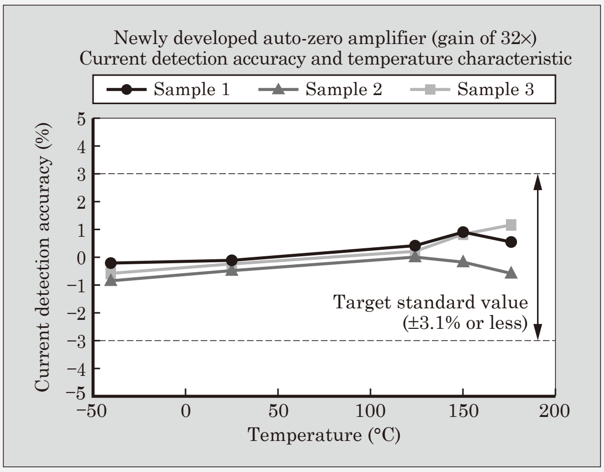

Fig.7 Evaluation results of an actual device using an auto-zero amplifier

3.7 Trench SBD-integrated SiC-MOSFET to suppress bipolar degradation

SiC has a higher breakdown electric field than Si and is capable of reducing the resistance of devices if the drift layer, which holds voltage, is made thinner and higher in carrier concentration. This means that it can contribute to loss reduction in power conversion equipment. Furthermore, SiC, which also has high heat conductivity and a wide band gap, enables devices to operate under high temperatures, allowing cooling systems to be simplified. With this advantage, it plays a role in the size and weight reduction of power conversion equipment.

On the other hand, loss is increased due to the increase in on-state voltage (bipolar deterioration) when current flows to the body diode functioning as the reverse-conducting device of the SiC-MOSFET. To counter this problem, we considered the integration of the SBD and MOSFET into one chip (trench SBD integration) as the bipolar deterioration suppression method.

In a Tsukuba Power-Electronics Constellations (TPEC) project, Fuji Electric has established the technology for forming a trench SBD in SiC trench gate MOSFETs. In the case of built-in trench SBDs, if trench SBDs are formed planarly between trench gates, the cell pitch must be wider than in conventional SiC trench-gate MOSFETs, resulting in increased conduction loss. In the project, we managed to form a trench SBD in the conventional SiC trench gate MOSFET, thereby achieving SBD integration without widening the cell pitch. In addition, narrower cell pitch caused less bipolar degradation and suppressed the loss increase.

Figure 8 shows the amount of change ΔV_F versus applied forward current density. In the graph, ΔV_F increases due to the bipolar current in the case of device B, which has a larger cell pitch, whereas

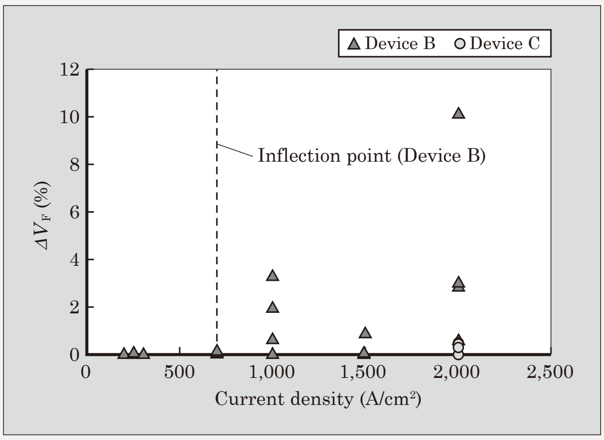

Fig.8 ΔV_F versus applied forward current density in the case of device C, which has a relatively narrower cell pitch, bipolar deterioration is suppressed, demonstrating that ΔV_F does not increase before a current density of 2,000 A/cm^2, which is the upper limit of the power supply system used. We also confirmed that bipolar deterioration can be suppressed stably regardless of the epitaxial substrate's threading basal plane dislocation (BPD) density (Refer to page 204, "Trench SBD-Integrated SiC-MOSFET To Suppress Bipolar Degradation").

4. Postscript

The above is a summary of Fuji Electric's latest developments in the field of power semiconductors. Since its foundation, Fuji Electric has pursued innovation in energy and environmental technologies, making a wide range of contributions to the world in such fields as industrial and social infrastructure and automobiles. Above all, power electronics is a field of technology that drives the rapidly growing efforts toward energy saving, decarbonization, and other environmental solutions. Power semiconductors are key devices in the field of power electronics, and by continuing to innovate the technology, Fuji Electric will continue to contribute to the creation of a responsible and sustainable society.

References

(1) Adachi, S. et at al. M677 100-kW Class Ultra-Compact IGBT Module for xEVs. FUJI ELECTRIC REVIEW. 2021, vol.67, no.4, p.232-235.

(2) Tateishi, Y. et at al. Cooling Technology for Ultra-Compact RC-IGBT Modules for xEVs. FUJI ELECTRIC REVIEW. 2021, vol.67, no.4, p.236-241.

(3) Branislav Stevanovic. et al. "Highly Efficient, Full ZVS, Hybrid, Multilevel DC/DC Topology for Two-Stage Grid-Connected 1500-V PV System With Employed 900-V SiC Devices". 2019, IEEE J. Emerg. Sel. Top. Power Electronics, vol.7, no.2, p.811-832.

(4) Iwasaki, Y. et al. All-SiC Modules with 2nd-Generation SiC Trench Gate MOSFETs. FUJI ELECTRIC REVIEW. 2019, vol.65, no.4, p.220-224.

(5) Minagawa, K. et al. 7th-Generation "X Series" IGBT-IPMs. FUJI ELECTRIC REVIEW. 2019, vol.65, no.4, p.210-214.

(6) Terashima, K. et al. 7th-Generation "X Series" IGBT-IPM with "P644" Compact Package. FUJI ELECTRIC REVIEW. 2020, vol.66, no.4, p.221-226.

(7) Minagawa, K. et al. "P631" Package 7th-Generation "X Series" High Power IGBT-IPM. FUJI ELECTRIC REVIEW. 2021, vol.67, no.4, p.247-251.

(8) Satou, K. et al. "The 7th Generation Intelligent Power Module for Industrial Applications". Proceeding of PCIM Asia 2021.

(9) Sekino, Y. et al. 3.3-kV SiC Hybrid High Power Modules for Railcars. FUJI ELECTRIC REVIEW. 2021, vol.67, no.1, p.66-68.

(10) Hiasa, N. et al. "FA8A80 Series" 650-V PWM Power Supply Control ICs. FUJI ELECTRIC REVIEW. 2017, vol.64, no.4, p.237-241.

(11) Nakagawa, S. et al. One-Chip Linear Control IPS, "F5106H". FUJI ELECTRIC REVIEW. 2013, vol.59, no.4, p.251-254.

(12) Toyoda, Y. et al. "60 V-Class Power IC Technology for an Intelligent Power Switch with an Integrated Trench MOSFET". ISPSD. 2013, p.147-150.

(13) Iwata, H. et al. "F5202H" 5th-Generation Intelligent Power Switch for Automotive Applications. FUJI ELECTRIC REVIEW. 2020, vol.66, no.4, p.206-210.

Package Technology for Achieving Higher Power Density in IGBT Modules for xEVs

SATO, Yushi* ADACHI, Shinichiro* HIGASHI, Nobuhiro*

ABSTRACT

In the automotive field, electrified vehicles are expected as a measure of reducing greenhouse gas emissions. Their power modules in the inverter are required to have a higher power density, that is, small, thin and high output. To meet these market demands, Fuji Electric has developed the "M677," an industry-leading ultra-compact IGBT module for xEVs. We have improved the short-circuit capacity of this small, thin IGBT by bonding the lead frame wiring on the flat surface of the chip to reduce the stress per unit volume that has increased with the growth of the power density. In addition, the solder joints have sufficient resistance to the electromigration lifetime to meet the market needs.

1. Introduction

In order to solve the issue of climate change, global efforts to reach carbon neutrality by the year 2050 are accelerating. In the automobile field, electrified vehicles powered by electric motors (xEVs), which include hybrid electric vehicles (HEVs), plug-in hybrid electric vehicles (PHEVs) and electric vehicles (EV), are considered to be one of the most effective ways to reduce greenhouse emissions.

To contribute to the fulfillment of this social demand, Fuji Electric has developed an industry-leading ultra-compact IGBT module, the "M677"[1],[2] (see Fig. 1) for xEVs, targeted for 100-kW class inverters as a key component of xEV power trains. The M677, which is designed to provide high power density, has successfully achieved a compact module size that meets the market demand.

This paper describes the packaging technologies that achieve higher power density.

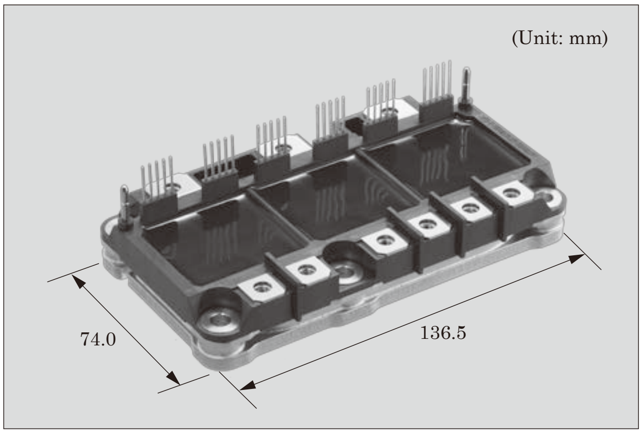

Fig.1 IGBT module M677 for xEVs

2. Challenges for Higher Power Density

To achieve reduced size and increased output power in the newly developed M677, we adopted the 7th-generation reverse conducting insulated gate bipolar transistor (RC-IGBT). And also in order to reduce conduction losses, we reduced the chip thickness and optimized the surface structure[1]. In addition, compared to the predecessor "M653," which is configured with two chips per arm*1, we achieved a smaller chip footprint with the new circuit configuration that uses one chip per arm. The result shows that the footprint of the main circuit has been reduced by half that of the predecessor M653, and as a consequence, the power density is almost double compared to the predecessor M653,[1],[2] as shown in Table 1. On the other hand, as an effect of the chip being made more compact and thinner than its predecessor, there is an inevitable decrease in thermal capacity due to the reduced chip

Table 1 Internal circuit comparison between the M653 and M677

	M653	M677
Internal circuit configuration	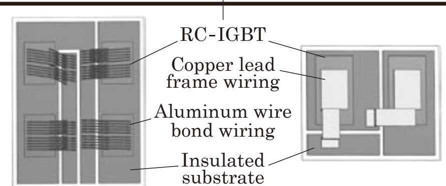	
Circuit area (arb. unit)	1.00	0.49
Power density (arb. unit)	1.00	1.98

* Semiconductors Business Group, Fuji Electric Co., Ltd.

*1 Arm: Refer to "Supplemental Explanation 1" on page 209 volume as well as an increase in thermal resistance due to the reduced surface area of the chip. Since the junction temperature must be kept below a specified value during operation to prevent module performance degradation, it is necessary to improve heat dissipation from the chip.

In addition, further measures against electromigration are required as power density increases. A phenomenon as electromigration in solder can occur when a high current flows in a narrow wiring area at high temperature. As metal atoms are transported by momentum exchange with conducting electrons, voids are formed, the increase of which leads to increased electrical and thermal resistance. As this can eventually lead to wire breakage, it is necessary to provide the high current density areas with adequate resistance to electromigration.

3. Improved Short-Circuit Capacity of Lead Frame in Thin Wafer RC-IGBTs

3.1 IGBT short-circuit failure modes

In power modules, short-circuit faults are caused by chip damage, abnormality in the control or driving circuit, malfunction due to noise, wire connection mistakes, ground fault, and other issues. In short circuit conditions, current conducting a chip raise up to is applied thousands of amperes of high with in a few microseconds while high voltage is being applied, and the IGBT will eventually fail if these conditions continue.

The IGBT failure modes associated with short-circuit faults can be divided into the four major modes shown in Fig. 2.[(4)-(8)] In mode A, a latch-up is caused by a high-amperage current when high voltage is being applied, and after turn-on, the IGBT fails immediately. In mode B, thermal destruction occurs due to rapid temperature rise caused by power loss during short-circuit operation. In mode C, destruction occurs due to the effect of current concentration caused by inhomogeneous operation inside the IGBT during turn-off operation. In mode D, the IGBT fails due to thermal runaway that occurs as a result of an abnormal leak current after a short circuit. The time an IGBT takes to fail when such short-circuit faults occur is defined as the short-circuit capacity.

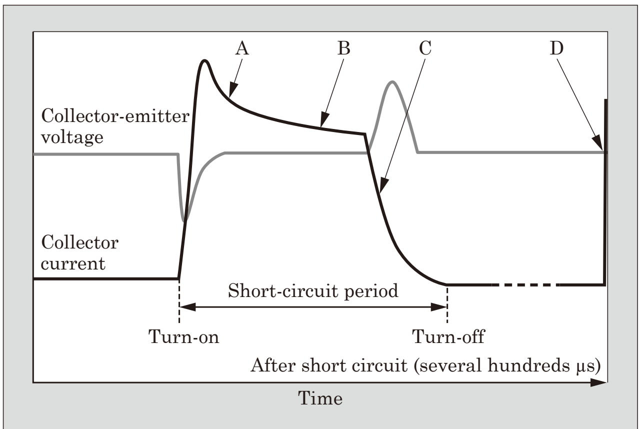

Fig.2 IGBT short-circuit failure modes

3.2 Relationship between the active volume of the IGBT and mode D short-circuit capacity

The cause of mode D short-circuit faults is the thermal runaway that occurs as a result of an abnormal leak current, which is produced after a short-circuit, causing the chip's internal temperature to rapidly rise.[(6)] This short-circuit capacity is reduced as the chip is made thinner. Thinner chips have a reduced volume and smaller thermal capacity, which is believed to be the reason why chip temperatures tend to rise dramatically against thermal runaway after a short circuit.[(9)] Figure 3 shows experiment results of between the active volume of an IGBT and short-circuit failure energy. The active volume of the IGBT is proportional to the short-circuit capacity with respect to mode D. In other words, size reduction and increased withstand capacity have a trade-off relationship.

3.3 Short-circuit capacity improved with lead frame wiring

While the thermal capacity decreases as chips are made thinner, the rise in temperature can be minimized by improving heat dissipation performance by increasing the area of the junction between the chip and the wiring.[(10)]

If the aluminum wire bond wiring used in the predecessor M653 is applied to the newly developed M677 chip, the short-circuit capability for mode D is 30% lower than that of the M653. To address this issue, we adopted a structure in which the copper lead frame wiring, which have a greater thermal capacity than aluminum wire bond wiring, are bonded to the chip's flat surface.

Figure 4 shows the comparison of short circuit capability between a wire bond wiring package and a lead-frame wiring package. Short circuit capability in the lead-frame wiring package dramatically increase

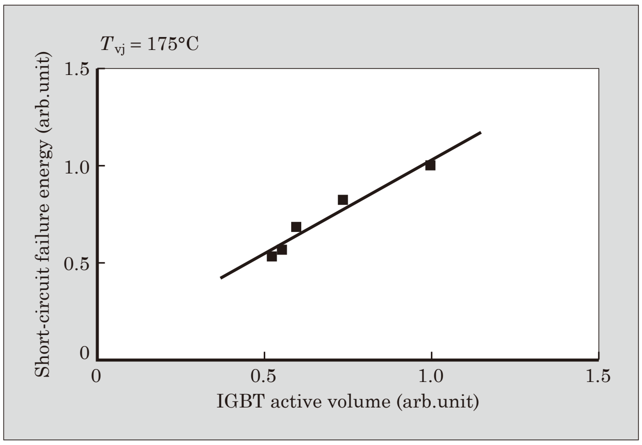

Fig.3 The experiment results of the relationship between IGBT active volume and short-circuit failure energy

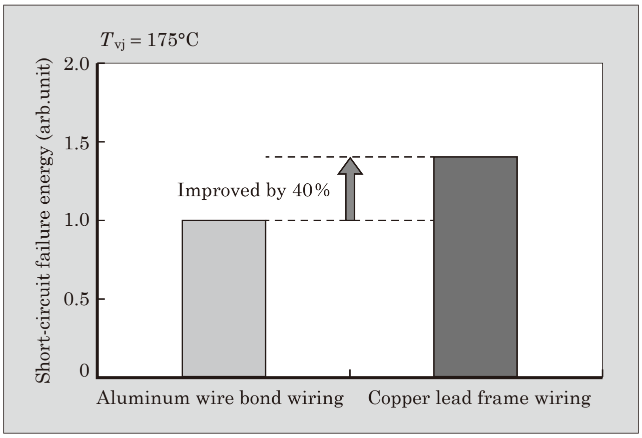

Fig.4 Effect of short-circuit capacity improved with lead frame wiring

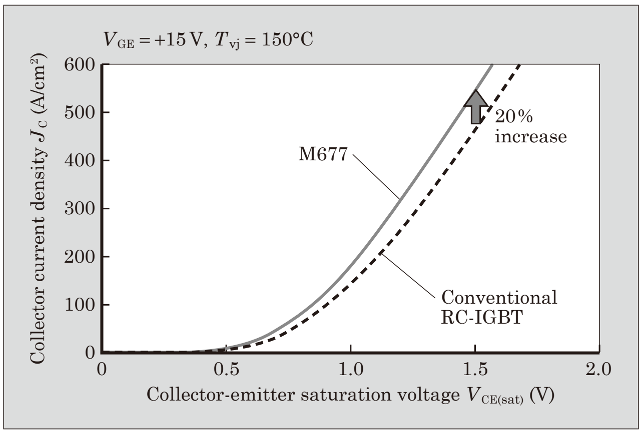

Fig.5 Collector-emitter saturation voltage $V_{CE(sat)}$

by 1.4 times compared to the one in the wire bond wiring package. The increase of short circuit capability allows to achieve the ruggedness to short circuit event in a thinner and smaller chip. The results show an improvement of 40% compared to the conventional aluminum wires.

In the M677, the measures above ensure short-circuit capability in thinner chips, which is effective in reducing conduction loss. In addition, the conduction loss has been reduced by optimizing the surface structure of the RC-IGBT. Figure 5 shows the collector-emitter saturation voltage $V_{CE(sat)}$. The collector-current density of M677 is higher than that of the conventional design by 20 % at the same saturation voltage.

4. Electromigration and Reliability Evaluation Method

4.1 Electromigration

The mean time to failure (MTTF) model of electromigration described in Chapter 2 can be estimated with the Black's equation shown in Equation (1) with current density and temperature as the main factors.[11]

$$\mathrm{MTTF} = AJ^{-n} \exp\left(\frac{Ea}{kT}\right) \quad \text{.................................(1)}$$

A : Constant
J : Current density
n : Current density exponent
Ea: Activation energy
k : Boltzmann constant
T : Absolute temperature

According to Equation (1), the MTTF due to electromigration is shorter at higher current densities and temperatures. Since among the components of power modules, the current density is greatest at the solder used as bonding material, we verified the electromigration resistance of the solder bonding areas during the development of the M677.

4.2 Effects of current density and temperature

We used test pieces that simulated the M677's solder bonding areas, which connect the lead frames and insulated substrate to the chip in order to evaluate their electromigration resistance. Figure 6 shows the overview of the test circuit. To decrease the distortion in the bonding areas caused by changes in temperature during power module operation, the M677 is designed with solders A and B, which have different characteristics, and in the test, we evaluated the test pieces for each of them.

In the test method we used, a constant current was continuously applied to the test pieces, and the ambient temperature was controlled in a temperature-controlled chamber. The current density and temperature, which are the determinants in the Equation (1) above, were compared as test conditions. Furthermore, as a criterion of electromigration lifetime, we used the time it takes for the resistance of the test piece to be increase by 20%.

As a result of the test, the electromigration lifetime with respect to current density is shown in Fig. 7, and the electromigration lifetime with respect to temperature is shown in Fig. 8. As was predicted by Black's

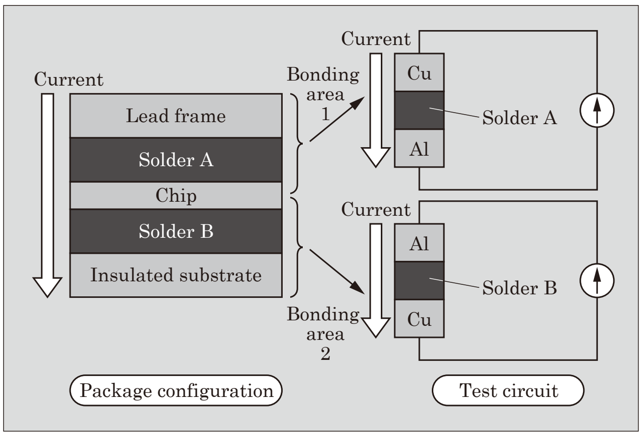

Fig.6 Test sample structures and set up in evaluation of electromigration

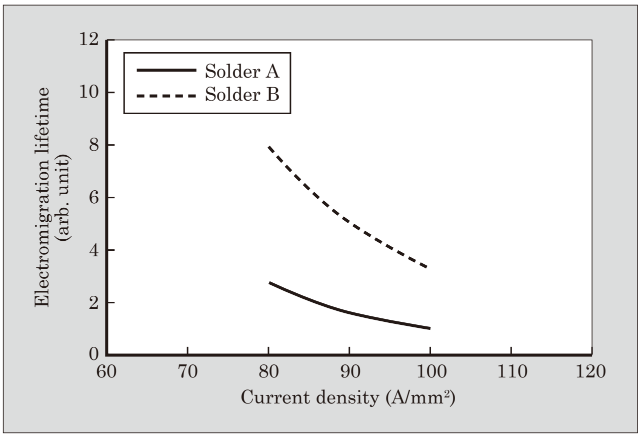

Fig.7 Current density dependence of electromigration lifetime

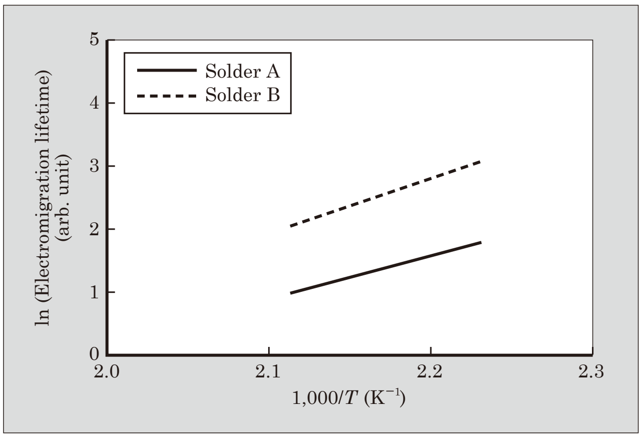

Fig.8 Temperature dependence of electromigration lifetime

equation, the electromigration lifetime is shorter at higher current densities and temperatures. We confirmed that solder B has a higher electromigration resistance than solder A.

4.3 Electromigration resistance of the M677

The M677's chip size, solder material, internal wiring and other features are designed to meet the target values for electromigration lifetime. The target electromigration lifetime was determined by the MTTF of the solder material obtained from Equation (1) based on the results for current density and temperature described in Section 4.2 and the stress expected when the power module is actually used in an xEV.

In verifying the electromigration resistance of the M677, we conducted a continuous heat run test with real equipment. Figure 9 shows the cross-sections of the solder bonding areas observed after the continuous heat run test. These are the cross-sections of solder bonding areas 1 and 2 after each of them were continuously subjected to currents for three times as long as the target lifetime. The cross-sections observed after the test showed no void caused by increases in wiring resistance or thermal resistance, and from these results, we determine that the M677 is durable enough to meet the target electromigration lifetime.

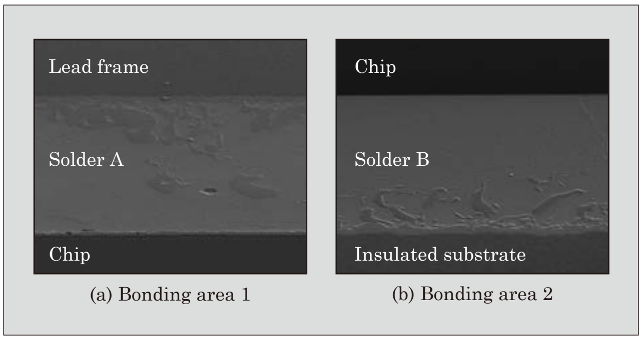

Fig.9 Solder bonding area cross-sections SEM image after the electromigration test in M677 tests

5. Postscript

This paper has described the improvement of short-circuit capacity and resistance to electromigration as part of our efforts to realize higher power density IGBT modules for xEVs. These efforts have made it possible for us to offer the "M677," the 100-kW class ultra-compact RC-IGBT module for xEVs.

We will continue developing technologies for lower power loss, higher power density, and higher reliability to meet the requirements for power semiconductors for xEVs, which will continue to growing rapidly, and by providing power modules that meet the market demand, we intend to contribute to the realization of carbon neutrality.

References

(1) Adachi, S. et at al. "M677" 100-kW Class Ultra-Compact IGBT Module for xEVs. FUJI ELECTRIC REVIEW. 2021, vol.67, no.4, p.232-235.

(2) Tateishi, Y. et at al. Cooling Technology for Ultra-Compact RC-IGBT Modules for xEVs. FUJI ELECTRIC REVIEW. 2021, vol.67, no.4, p.236-241.

(3) Arai, H. et al. 3rd-Generation Direct Liquid Cooling Power Module for Automotive Applications. FUJI ELECTRIC REVIEW. 2015, vol.61, no.4, p.252-257.

(4) Yamashita, J. et al," A Study on the Short Circuit Destruction of IGBTs", Proc. of the 5th ISPSD, 1993, p.35-40.

(5) Yamashita, J. et al," A Study on the IGBT's Turn-off Failure and Inhomogeneous Operation", Proc. of the 6th ISPSD, 1994, p.45-50.

(6) Otsuki, M. et al, "Investigation on the Short-Circuit Capability of 1200 V Trench Gate Field-Stop IGBTs", Proc. of the 14th ISPSD, 2002, p.281-284.

(7) Hagino, H. et al, "An Experimental and Numerical Study on the Forward Biased SOA of IGBT's", IEEE Transactions. Electron Devices, 1996, vol.43, no.3, p.490-500.

(8) Takata, I. et al, "Non Thermal Destruction Mechanisms of IGBTs in Short Circuit Operation", Proc. of the 14th ISPSD, 2002, p.173-176.

(9) Otsuki, M. et al, "A Study on the Short-Circuit Capa-

bility of Field-Stop IGBTs", IEEE Transactions. Electron Devices, 2003, vol.50, no.6, p.1525-1531.
(10) Otsuki, M. et al, "Advanced thin wafer IGBTs with new thermal management solution", ISPSD, 2003, April 14-17, Cambridge UK, p.144-147.
(11) R. L. de Orio. et al, "Physically based models of electromigration: From Black's equation to modern TCAD models", Microelectronics Reliability, 2010, vol.50, p.775-789.

Line-Up Expansion of 2nd-Generation 1,700-V All-SiC Modules

TAKAKU, Taku* TAKASAKI, Aiko* OKUMURA, Keiji*

ABSTRACT

Fuji Electric has developed 1,200-V All-SiC modules, which are expected to significantly reduce dissipation losses of power converters compared with silicon (Si) power semiconductors. We have newly developed an All-SiC module equipped with a 1,700-V SiC-MOSFET using the 2nd-generation trench gate structure. It is designed for high-voltage power converters used in motor drives, renewable energy and traction. The All-SiC modules reduce dissipation losses in the power converters by 68% compared with Si-IGBT modules with the same power ratings. It is expected to increase the density and miniaturization of the power conversion systems.

1. Introduction

To realize a sustainable society, it is vital to pursue carbon neutrality by making energy use more efficient, reducing energy consumption, and expanding photovoltaic (PV), wind, and other forms of renewable energy. To achieve this, the efficiency of power converters, which are essential for the generation and conversion of electricity, and the power semiconductors that are their components needs to be improved. Currently, the characteristics of Si devices, which are the mainstream power semiconductors, are approaching their physical limits, making it difficult to significantly improve their efficiency. Under these circumstances, the application of SiC devices is expanding as a means to further improve the efficiency and energy-saving performance of power conversion systems.

Previously, Fuji Electric has developed All-SiC modules for industrial applications rated at 1,200 V, 300 to 600 A, using the 2nd-generation SiC trench gate metal-oxide-semiconductor field-effect transistor (MOSFET).

On the other hand, power semiconductor modules rated at 1,200 V do not have sufficient blocking voltage for the power converters with a DC bus voltage of 900 to 1,100 V used for 690-V AC motor drives and traction. Moreover, there is a movement in renewable energy applications, such as PV and wind, to increase the DC bus voltage from 1,000 to 1,500 V to improve the efficiency and reduce the costs.[(2)] Therefore, neutral-point-clamped three-level inverter circuits are often used and power semiconductors with a blocking voltage of 1,700 V are applied.

Fuji Electric has developed a 1,700-V All-SiC module mounted with a 2nd-generation SiC trench gate MOSFET for industrial applications that require a high blocking voltage.[(3)]

This paper presents the All-SiC modules rated at 1,700 V as a new series of products.

2. Characteristics of the 1,700-V All-SiC Module

2.1 2nd-generation 1,700-V SiC trench gate MOSFETs

Figure 1 shows the circuit configuration and external appearance of the 1,700-V All-SiC module developed in this project. The module has a half-bridge circuit configuration, in which the 2nd-generation 1,700-V SiC trench gate MOSFETs (SiC-MOSFETs) and 1,700-V Schottky barrier diodes (SiC-SBDs) are connected in anti-parallel, and the two pairs are connected in series. The 1,700-V SiC-MOSFET suppresses the increase of on-state resistance and ensures long-term reliability by optimizing the drift layer and the junction field-effect transistor (JFET) width in the 2nd-generation 1,200-V SiC trench-gate MOSFET technology.[(3)]

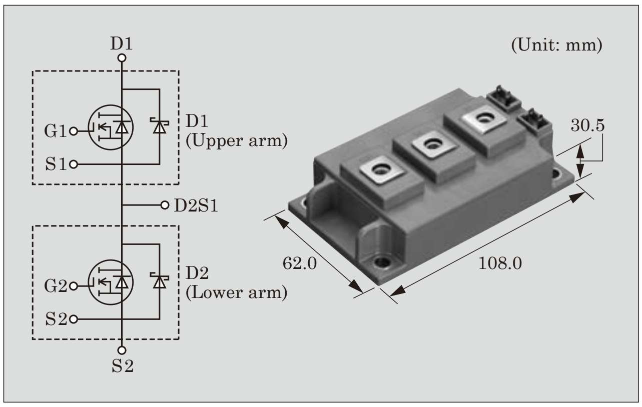

Fig.1 Circuit configuration and external appearance of the 1,700-V All-SiC module

* Semiconductors Business Group, Fuji Electric Co., Ltd.

2.2 New structure "M295" package[4]

SiC-MOSFETs are majority carrier (unipolar) devices, and they are capable of faster switching than Si-insulated gate bipolar transistors (IGBTs), which are minority carrier (bipolar) devices. However, under high-speed switching conditions, it has the disadvantage of causing high surge voltages due to the wiring inductance inside the module. To solve this problem in the new line-up of the All-SiC modules, the wiring inductance has been reduced by 24% by using a laminated bus bar structure for the internal P and N terminals, as shown in Fig. 2. Furthermore, this package makes it easier to replace from Si-IGBTs, as the external dimensions and the terminal layout are compatible with a 2-in-1 package "M276" of the 7th-generation "X Series" IGBT.

2.3 Output characteristics

Figure 3 shows a comparison of the output characteristics of the All-SiC module using 2nd-generation SiC trench gate MOSFETs and the conventional 7th-generation X-Series Si-IGBT module rated at 1,700 V/300 A. The All-SiC modules are composed of MOSFETs, which are unipolar devices, and therefore do not have the built-in voltage found in IGBTs, which are bipolar devices. The on-state voltage V_{DS} of the All-SiC module is lower than the on-state voltage V_{CE} of the Si-IGBT module, and the V_{DS} is 0.4 V at I_D = 150 A.

In general, the RMS current of a power conversion system is often designed to be 30% to 50% of the rated current of the power semiconductor module. Therefore, in the case of I_D = 150 A, the conduction loss of the All-SiC module can be reduced by 33% in comparison with the Si-IGBT modules with same rated current.

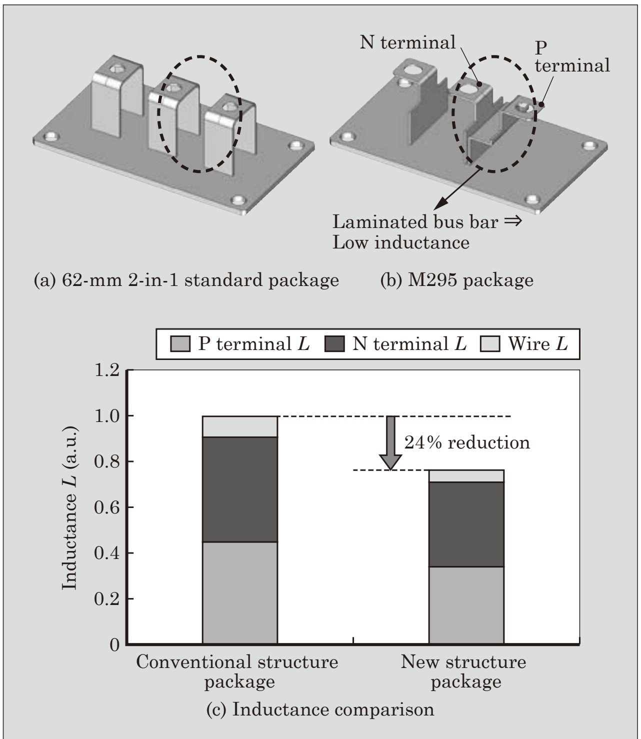

Fig.2 Internal package structure

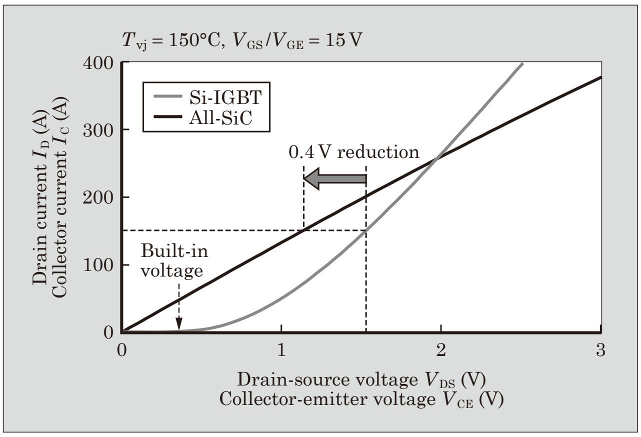

Fig.3 Comparison of output characteristics

2.4 Switching characteristics

To clarify the difference in the switching loss characteristics between the All-SiC module and the conventional Si-IGBT module, the switching waveforms were compared at the same turn-off dv/dt and turn-on di/dt conditions. Table 1 shows the gate resistance R_G values for the turn-off dv/dt and the turn-on di/dt.

Figures 4(a), 4(b), and 4(c) show the comparisons of switching waveforms of the All-SiC and the Si-IGBT modules at a rated current of 300 A under the conditions listed in Table 1.

The All-SiC module has a significantly reduced tail current during turn-off and reverse recovery compared with the Si-IGBT module [see Figs. 4(a) and (c)]. The peak currents during turn-on and reverse recovery are also significantly reduced [see Figs. 4(b) and (c)]. In the case of the Si-IGBT module, which is a bipolar device, the excess carriers caused by a minority carrier injection affect the switching operation, whereas in the case of the All-SiC module, which is a unipolar device, the operation is with majority carriers only.

In addition, as shown in Fig. 4(a), the turn-off surge voltage of the All-SiC module is kept at a low level even though the di/dt value of the All-SiC module is larger than that of the Si-IGBT module. This is due to the effect of the reduced internal inductance of the new package developed for the All-SiC as described in Section 2.2.

Table 2 shows a comparison of turn-off loss E_{off},

Table 1 Turn-off dv/dt and turn-on di/dt

Switching condition T_{vj} = 175°C	Turn-off		Turn-on	
	R_G (Off)	dv/dt	R_G (On)	di/dt
Si-IGBT	0.39 Ω	4.19 V/ns	0.39 Ω	3.28 A/ns
All-SiC	27 Ω	4.15 V/ns	3 Ω	3.48 A/ns

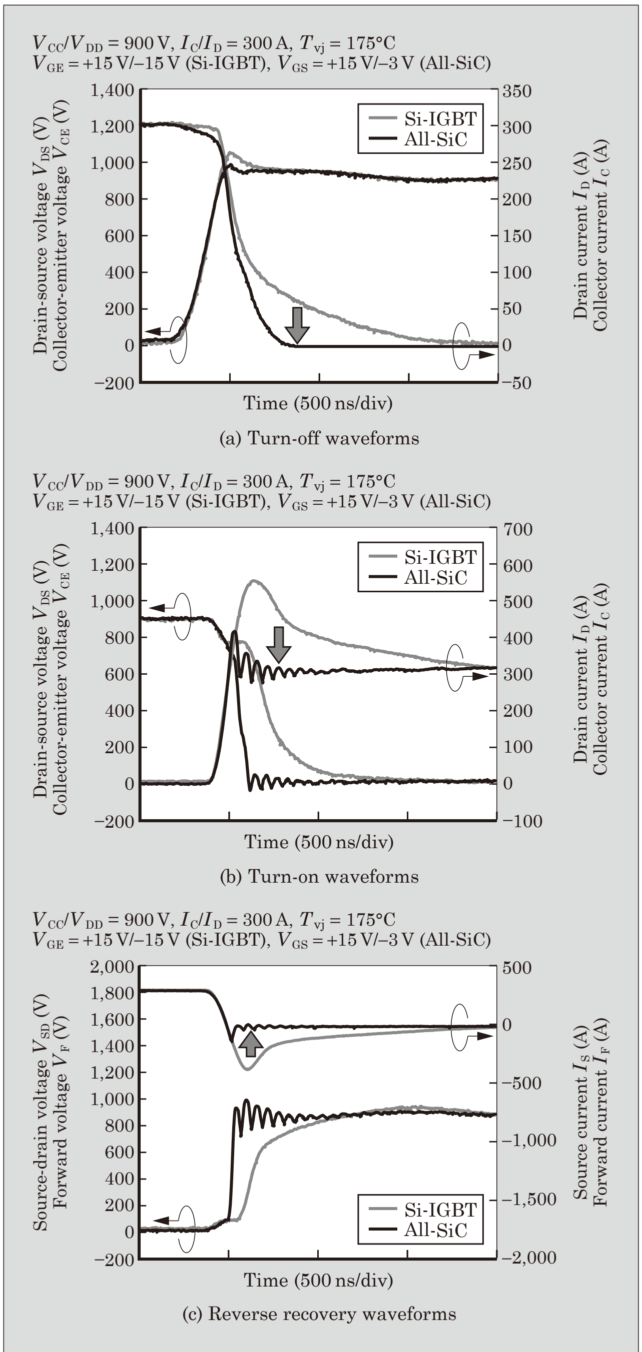

Fig.4 Switching waveform comparison between All-SiC and Si-IGBT modules

Table 2 Switching loss comparison

Switching condition T_{vj} = 175°C	Turn-off loss E_{off}	Turn-on loss E_{on}	Reverse recovery loss E_{rr}	Total
Si-IGBT	96.0 mJ	109.1 mJ	98.4 mJ	303.5 mJ
All-SiC	61.1 mJ	24.6 mJ	0.98 mJ	86.7 mJ
Reduction	36%	77%	99%	71%

turn-on loss E_{on} and reverse recovery loss E_{rr} of the All-SiC module and the Si-IGBT module. The E_{off}, E_{on} and E_{rr} of the All-SiC module are reduced by 36%, 77% and 99%, respectively, compared with those of the Si-IGBT module.

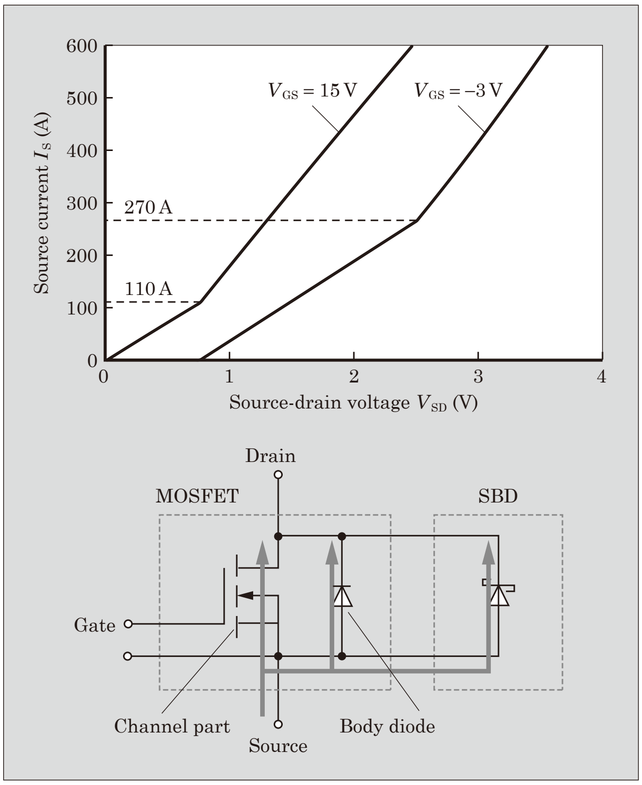

Fig.5 Source current output characteristics

As a result, total switching loss of the All-SiC module is reduced by 71% compared with the Si-IGBT module under the same switching speed condition.

2.5 Reverse output characteristics

Current (source current I_S) flows to the SiC-MOSFET in the opposite direction to that of the drain current when an inductive load current is turned off. Figure 5 shows the output characteristics under these conditions. Because the newly developed All-SiC module has SiC-SBDs connected in anti-parallel configuration to the SiC-MOSFET, the output characteristic has an inflection point because it is a combination of the characteristics of the SiC-MOSEFT's body diode (BD) and the SiC-SBD.(5) In the case where the gate-source voltage V_{GS} is −3 V, the current flows through the SiC-SBD only when the I_S is below the inflection point of 270 A. The current is split between the BD and SBD of the MOSFET when the current exceeds 270 A. Meanwhile, the V_{GS} is 15 V, the current flows the MOSFET's channel only when I_S is at or below the inflection point of 110 A, and the current flow splits to the MOSFET and SBD when the current exceeds 110 A.

3. Simulation Result of Dissipation Losses for Power Converters

We simulated the dissipation losses of the All-SiC module applied to the neutral point clamped (NPC)

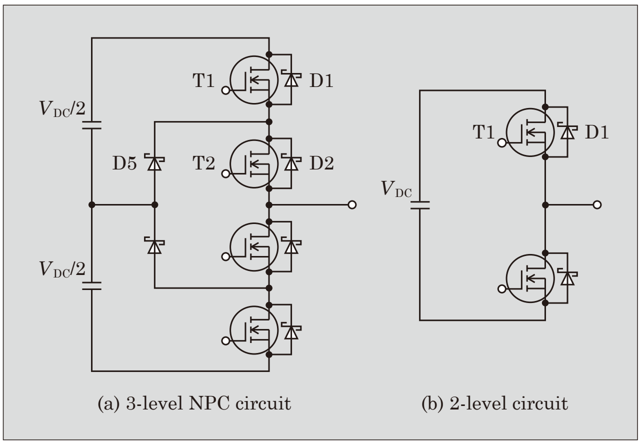

Fig.6 3-level and 2-level inverter circuits

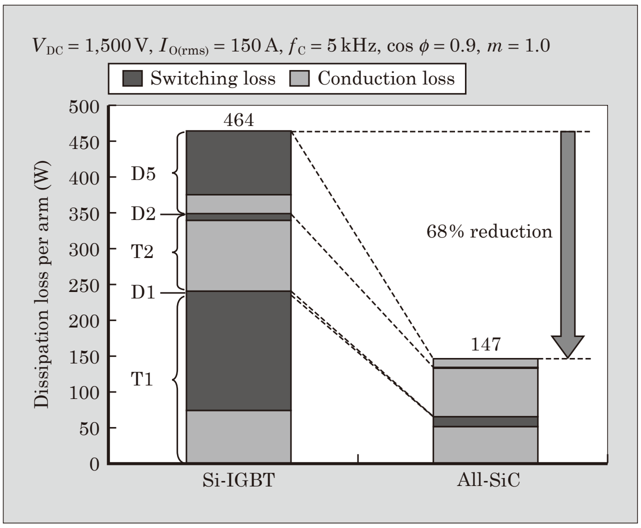

Fig.7 Loss comparison with a 1,500-V DC 3-level inverter circuit

circuit as shown in Fig. 6(a) in power converters with a DC bus voltage of 1,500 V and an output current of 150 A, as seen in PV and wind power generation. Figure 7 shows a comparison of the losses of the 1,700-V/300-A All-SiC module and the same rated Si-IGBT module. The All-SiC module has a 68% lower total inverter loss due to the significant reduction in switching losses at T1 and D5. This suggests that the size of the heatsink required for cooling can be reduced to approximately one-third, resulting in a significant reduction in the size of the inverter and higher efficiency.

Figure 8 compares the losses of a 3-level circuit and a 2-level circuit in power converters with a DC bus voltage of 1,100 V. For the Si-IGBT module, the following two cases were compared: a 1,200-V module in a 3-level NPC circuit shown in Fig. 6(a) and a 1,700-V module in a 2-level circuit shown in Fig. 6(b). By changing the configuration from the 3-level circuit with the 1200-V Si-IGBT to the 2-level circuit with the 1,700-V Si-IGBT, the number of semiconductor devices is reduced but the total loss is increased because of the large switching losses. On the other hand, the 2-level circuit with the 1,700-V All-SiC module significantly reduces the switching loss and consequently reduces the total loss by 69% compared with the 3-level circuit. This result shows that the 1,700-V All-SiC module can not only achieve higher efficiency but also can simplify a power conversion system with a DC bus voltage of 1,100 V by reducing the number of required power semiconductor devices and drive circuits, from 10 to 4 and from 4 to 2, respectively.

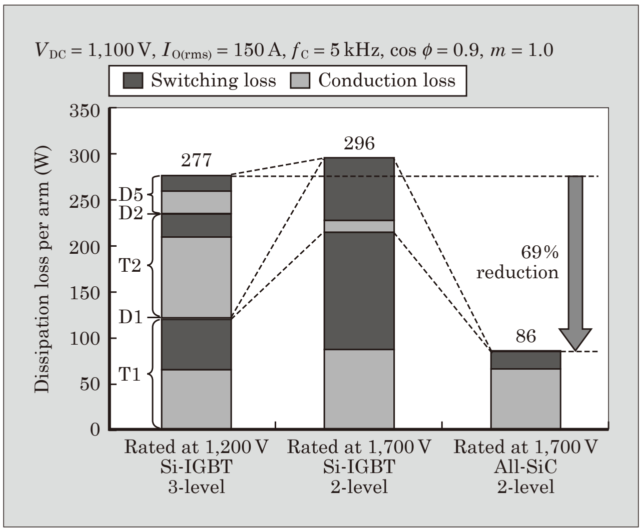

Fig.8 Loss comparison with 3-level and 2-level circuits

Table 3 "M295" package All-SiC module line-up

MOSFET generation	Package	Circuit	Rated voltage	Rated current
2nd generation trench gate	M295 	2 in 1	1,200 V	300 A
				450 A
				650 A
			1,700 V	200 A
				300 A
				400 A

4. All-SiC Module Line-Up

Table 3 shows the product line-up of the M295 package All-SiC modules. The new 1,700-V rated products with rated currents from 200 to 400 A use the same M295 package as the existing 1,200-V rated products. The M295 package is compatible with the 7th-generation X-Series IGBT modules and it can be applied to various types of power converters.

5. Postscript

This paper has described the newly developed All-SiC modules with a rated voltage of 1,700 V. These new products are expected to enable higher efficiency, higher power density and smaller size of power conversion systems for the markets that have grown significantly in recent years such as renewable energy and traction.

We will develop other All-SiC modules with different ratings and packages in order to meet varied market demands and contribute to the creation of a sustainable society.

References

(1) Yoshida, T. et al. "FRENIC-eFIT" Environmentally Resistant Inverter Designed for Harshest Installation Conditions. FUJI ELECTRIC REVIEW. 2018, vol.64, no.1, p.16-20.

(2) Stevanovic, B. et al. "Highly Efficient, Full ZVS, Hybrid, Multilevel DC/DC Topology for Two-Stage Grid-Connected 1500 V PV System with Employed 900 V SiC Devices". 2019, IEEE J. Emerg. Sel. Top. Power Electronics, vol.7, no.2, p.811-832.

(3) Iwasaki, Y. et al. All-SiC Modules with 2nd-Generation SiC Trench Gate MOSFETs. FUJI ELECTRIC REVIEW. 2019, vol.65, no.4, p.220-224.

(4) Takasaki, A. et al. 1,200-V 2nd-Generation All-SiC Modules. FUJI ELECTRIC REVIEW. 2020, vol.64, no.4, p.216-220.

(5) Uchida, T. et al. 2nd-Generation 1,700-V SiC Trench Gate MOSFETs. FUJI ELECTRIC REVIEW. 2021, vol.67, no.4, p.268-272.

Line-Up of Compact 7th-Generation IGBT-IPMs with RC-IGBTs

KUROSAWA, Eiji* JOZUKA, Naohiko* KARAMOTO, Yuki*

ABSTRACT

In order to meet the demand for further miniaturization and higher reliability in power conversion systems, Fuji Electric has developed a line-up of the 7th-generation IGBT-IPMs that is equipped with RC-IGBT chips and uses the new compact "P639" package, the footprint of which is 27% smaller than that of "P629" package used for 6th-generation IGBT-IPMs. By applying the 7th-generation chip technology and new control technology for driving the IGBT, the new compact P639 has reduced the power dissipation during continuous operation by 7%. Moreover, it applies the 7th-generation packaging technology to achieve high-temperature operation at 150°C.

1. Introduction

With the widespread adoption of factory automation and communication devices including mobile phones in recent years, the demand for servo systems used for industrial robots, machine tools and other applications has been increasing. These kinds of equipment are strongly required to save space. Since the power semiconductors used in them also need to be miniaturized, high temperature operation and low power dissipation of semiconductors are quite important to achieve this requirement. In addition, they are expected to be highly reliable in order to prevent sudden failures.

IGBT-IPMs have gate driving and protection circuits. IGBT IPMs are used in a wide variety of applications, including NC machine tools, robots and elevators that require particularly high reliability.

For 7th-generation IGBT-IPM(1)-(4), which is the latest generation of IGBT-IPM, Fuji electric has applied 7th-generation chip technology, in which the finer IGBT trench gate structure and the thinner drift layer stemmed from a thin wafer processing technology are adopted to achieve low power dissipation. In addition to that, Fuji electric has adopted a new control technology to drive the IGBT optimally. Furthermore, the IGBT-IPM has realized higher temperature operation by applying the 7th-generation packaging technologies such as high heat resistant gel and highly reliable solder. In order to meet the demand for further size reduction and high reliability, Fuji Electric has added a new product to the existing 7th-generation IGBT-IPM line-up, which is equipped with the new compact package "P639" with reverse conducting IGBT (RC-IGBT) chips(5). This product has high heat dissipation characteristics and high-precision protection function that directly detects the characteristics of IGBT chips. As a result, it has achieved the industry-leading size reduction. It will contribute to the miniaturization of the systems.

2. Features

2.1 Overview of product

Figure 1 shows the external appearance of the new compact P639 package. The external dimensions of the P639 package are D36.0 × W70.0 × H12.0 (mm), and it features a 6-in-1 circuit configuration, which integrates a three-phase inverter circuit into one module. The P639 achieves its compactness by incorporating an RC-IGBT chip.

Table 1 shows the line-up of the 7th-generation IGBT-IPM and the previous 6th-generation IGBT-IPM at ratings of below 650 V/50 A and 1,200 V/25 A. The 6th-generation IGBT-IPM line-up only includes the "P629" package, which is equipped with the pre-

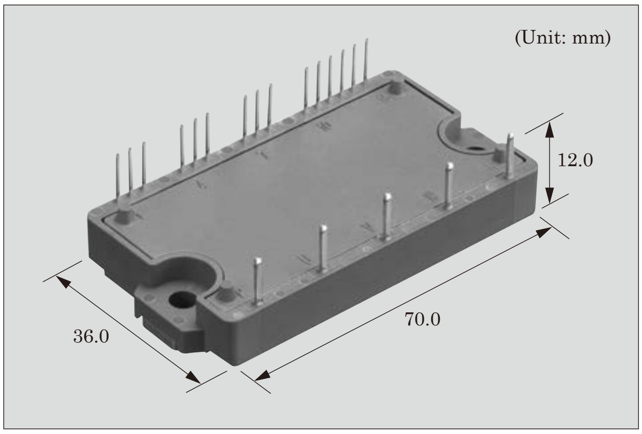

Fig.1 Appearance of the new compact package "P639"

* Semiconductors Business Group, Fuji Electric Co., Ltd.

Table 1 Product line-up

Rating		6th-generation IGBT-IPM	7th-generation IGBT-IPM
650 V	1,200 V		
20 A	10 A	P629	P639
30 A	–		
50 A	25 A		P629

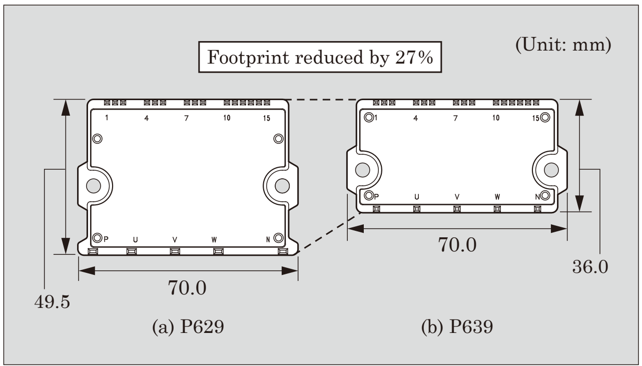

Fig.2 Comparison of external dimensions between the “P629” and “P639”

vious IGBT chip. On the other hand, 7th-generation IGBT-IPM line-up, which includes the more compact P639 package models, contributes to size reductions in equipment.

Figure 2 shows a comparison of the external dimensions between the P629 and P639. The P639 has a 27% smaller footprint compared to the P629. Furthermore, it is easy to replace the P629 with the P639 due to the same arrangement of the main and control terminals.

The new compact P639 has reduced the power dissipation by 7% compared to the previous 6th-generation IPM by applying the 7th-generation chip technology and the new control technology. Furthermore, the 7th-generation packaging technology enables higher temperature operation. Moreover, by using RC-IGBT chips, which can reduce chip temperature swing during low-frequency operation, the ΔT_{vj} power cycling lifetime has been improved in comparison with the product mounted with the 6th-generation IGBT and free wheeling diode (FWD) chips.

2.2 Product features

(1) Package size reduction

Since the chip mounting area occupied approximately 30% of the total area in the conventional P629, it is important to reduce the chip size in order to achieve the miniaturization of the product. However, the chip characteristic, such as thermal resistance will get worse as the chip size shrinks. In addition, it may lead to the decrease in the reliability when the number of aluminum wires is reduced. In order to solve these issues, the new compact P639 has applied RC-IGBT chips.

Figure 3 shows the schematic diagram and the equivalent circuit diagram of the RC-IGBT chip. As mentioned above, an IGBT and a FWD are integrated on the same RC-IGBT chip, and the area of the RC-IGBT chip is smaller than the combined area (total area) of the 6th-generation IGBT and FWD chips.

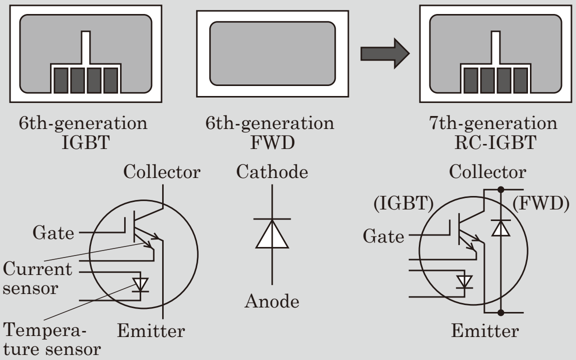

	IGBT + FWD	RC-IGBT
Footprint ratio	0.9 + 0.6 = 1.5	1

Fig.3 Schematic diagrams and equivalent circuit diagrams of the RC-IGBT chip

Table 2 Comparison between 6th- and 7th-generation chips at 650V/20A

Item	6th-generation IGBT + FWD	7th-generation RC-IGBT
Total chip area ratio	IGBT + FWD 0.9 + 0.6 = 1.5	1.0 (–33%)*
Number of aluminum wires	4	4
FWD thermal resistance (°C/W)	1.96	1.21 (–38%)*

*Rate of reduction from the 6th generation

Table 2 shows a comparison between the 6th-generation and the 7th-generation chips with a rating of 650 V/20 A. The 7th-generation IGBT-IPM’s total chip area is reduced by 33% compared to the 6th-generation IGBT-IPM. Since the chip area of the 7th-generation RC-IGBT is larger than that of each individual 6th-generation IGBT and FWD, the same number of aluminum wires can be bonded. Furthermore, the thermal resistance is reduced by 38% due to the increased chip size, and for this reason, it is expected to have better heat dissipation performance. As a result of these features, the new compact P639 has achieved size reduction without sacrificing the product characteristics and reliability.

(2) ΔT_{vj} power cycling lifetime improvement

The ΔT_{vj} power cycling lifetime is a important lifetime characteristic of the power modules described in this paper. This is defined by the number of repeated temperature swing ΔT_{vj} permissible for the chip. The product will break down if ΔT_{vj} is repeated for more than the capability. This is because thermal stress caused by ΔT_{vj} causes the degradation in the chip-aluminum wire and chip-solder bonding areas. In addition, the ΔT_{vj} power cycling lifetime depends on the magnitude of ΔT_{vj} and therefore decreases when ΔT_{vj} is higher.

NC machine tools and other devices have some modes in which low frequencies are used for low-speed or high-torque operation. At low-frequency operation, the chip temperature is prone to rise because current flows through the IGBT or FWD in the same phase for a long time. On the other hand, since the time during which no current flows is also long, causing the chip temperature decreases during this period. Therefore, the ΔT_{vj} of the chip is higher and the thermal stress produced is also higher, resulting in shorter ΔT_{vj} power cycling lifetime.

Figure 4 shows the calculation results of chip temperature swing at low-frequency operation. The 6th-generation IGBT-IPM equipped with conventional IGBT and FWD chips has a higher ΔT_{vj} depending on the presence of the heat generation period because the IGBT chip and the FWD chip generate heat alternately during inverter operation. As a result, ΔT_{vj} of the IGBT is 24°C and that of FWD is 28°C. On the other hand, the 7th-generation IGBT-IPM equipped with RC-IGBT chips features reduced changes in chip temperature because the RC-IGBT generates heat in the IGBT region and the FWD region alternately within one chip. In addition, the increase of chip temperature is suppressed due to the improved thermal resistance. As a result of this feature, the ΔT_{vj} of the 7th-generation IGBT-IPM's RC-IGBT chip is 7°C lower than that of the FWD chip, in which the temperature swing is larger when used in combination with the IGBT chip in the 6th-generation IGBT-IPM combination. Figure 5 shows the ΔT_{vj} power cycling lifetime curve. In this example, the ΔT_{vj} power cycling lifetime of the 7th-generation IGBT-IPM estimated to be

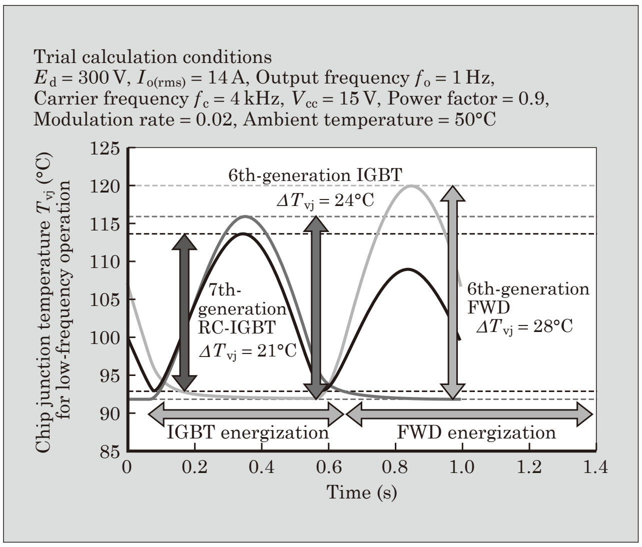

Fig.4 Trial calculation results of changes in chip temperature at low-frequency operation

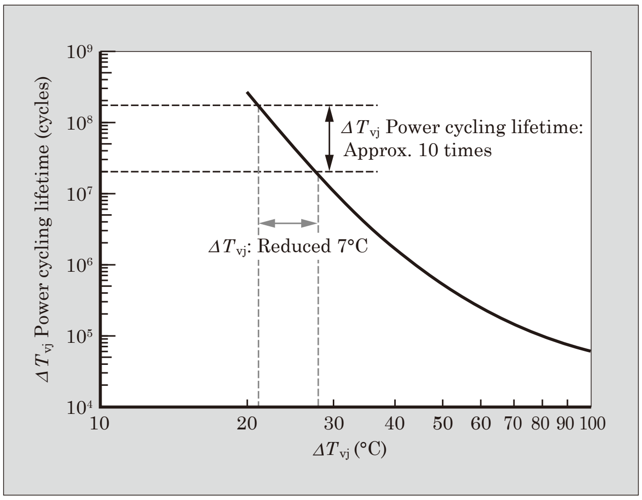

Fig.5 ΔT_{vj} Power cycling lifetime curve

approximately 10 times higher than that of the 6th-generation IGBT-IPM.

(3) Reduction of power dissipation

(a) IGBT saturation voltage and turn-off energy

The 7th-generation IGBT features improved trade-off characteristics between collector-emitter saturation voltage $V_{CE(sat)}$ and turn-off energy E_{off} due to the finer pattern of the surface trench gate structure and the thinner drift layer achieved through the use of thin wafer processing technology.[1],[6] For this reason, the newly developed RC-IGBT chip mounted on the P639 has reduced $V_{CE(sat)}$ by 0.05 V and E_{off} by 0.14 mJ compared to those of the conventional 6th-generation IGBT chip, as shown in Fig. 6.

(b) Turn-on energy

Figure 7 shows the current dependency of turn-on energy E_{on} for the 650-V/20-A 7th-generation IGBT-IPM. In order to reduce E_{on}, the P639 has adopted a new control technology for the IGBT drive control. In general, the dv/dt of IGBT chips at turn-on decreases as the chip junction tempera-

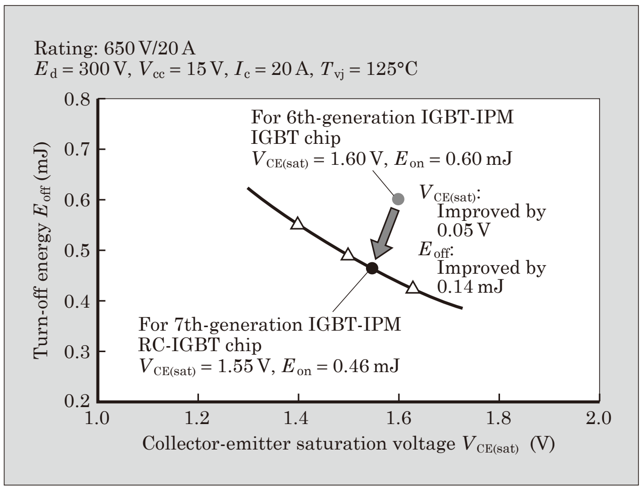

Fig.6 Trade-off relation between collector-emitter saturation voltage and turn-off energy

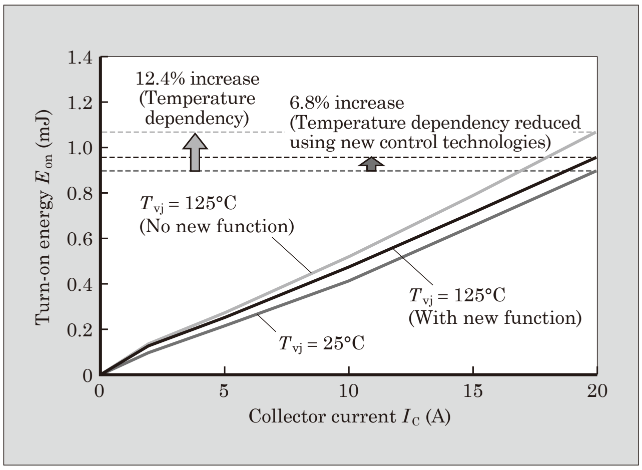

Fig.7 Collector current dependency of the turn-on energy

ture increases. Therefore, E_{on} increases as the chip temperature rises. As a result, in the case of 650 V/20 A with the conventional control technique applied, E_{on} at the rated current condition increases by 12.4% at a high temperature (125°C) compared to a room temperature (25°C). On the other hand, thanks to the new control technique, the 7th-generation IGBT-IPM optimizes the dv/dt by increasing turn-on gate drive current when the IGBT chip temperature rises. By feeding back the temperature measured by the temperature sensor formed on the IGBT chip to the gate drive circuit, the gate drive current is adjusted to optimally control dv/dt. With this new function, the increase of E_{on} at 125°C can be reduced by 6.8% compared to E_{on} at 25°C.

(c) Power dissipation during inverter operation

Figure 8 shows the simulation results of power dissipations per arm* for the 7th-generation IGBT-IPM and the 6th-generation IGBT-IPM in a three-phase inverter system. The rating of both IPMs is 1200 V/200 A. The 7th-generation P639 has

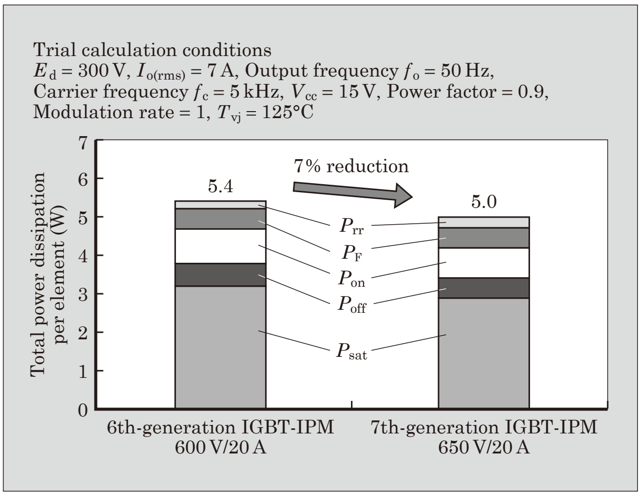

Fig.8 Comparison of total power dissipation

* Arm: Refer to page 209, "Explanation 1."

reduced the power dissipation by 7% compared to the 6th-generation IGBT-IPM, due to the improved trade-off characteristics between $V_{CE(sat)}$ and E_{off} and the reduction of E_{on}.

(d) Heat dissipation performance

As shown in Fig. 9, the footprint of the copper base, which has the role to facilitate the heat dissipation, has been reduced by 32% for the P639 compared to the P629 in order to make the package more compact, and as a consequence, the heat dissipation performance has become worse. Figure 10 shows the results of temperature distribution analysis of the copper base using the finite element method (FEM), in which heatsink dissipation performance and power dissipation were analyzed under the same conditions. Compared to that of the P629, the temperature change ΔT_c in the P639 increased by 6% due to the reduction in the surface area of the copper base.

However, the new compact P639 has reduced the power dissipation by 7% compared to the 6th-generation IGBT-IPM as mentioned before. There-

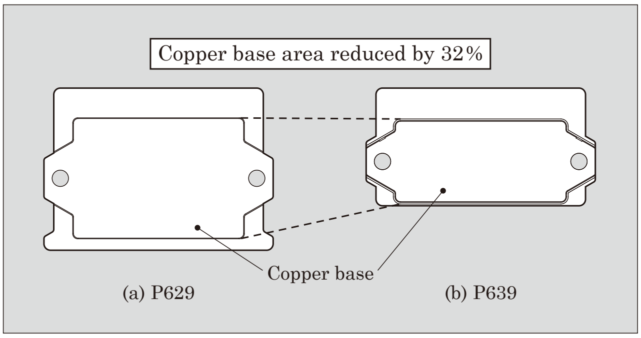

Fig.9 Comparison of copper base size

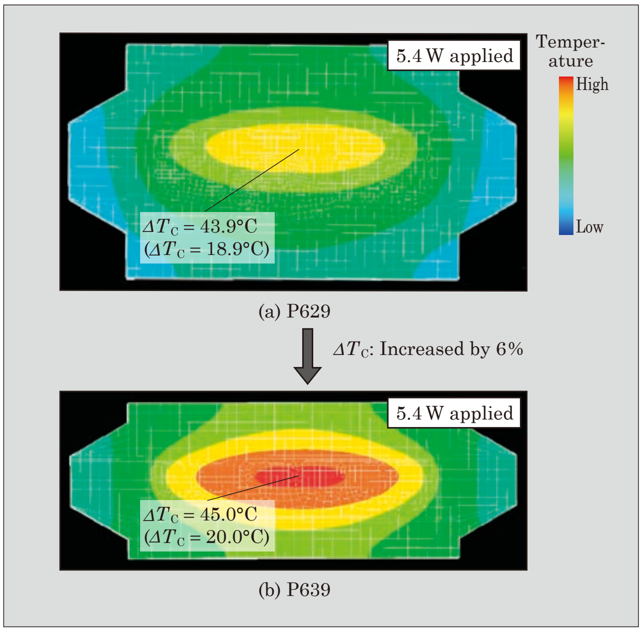

Fig.10 FEM analysis results of copper base temperature distribution

Table 3 Comparison of permissible operating temperatures

Item	6th-generation IGBT-IPM	7th-generation IGBT-IPM
Maximum case temperature T_{cmax}	110°C	125°C
Maximum junction temperature during continuous operation T_{vjop}	125°C	150°C
Maximum junction temperature T_{vjmax}	150°C	175°C

fore, in spite of the increase in ΔT_c caused by the reduction of the copper base size, it is possible to surpress the chip temperature to the same level as the 6th-generation IGBT-IPM. For this reason, the 7th-generation IGBT-IPM can easily replace conventional products.

(4) High temperature operation

Table 3 shows the permissible operating temperatures between the 7th-generation and 6th-generation IGBT-IPMs. The 7th-generation IGBT-IPM has expanded the maximum junction temperature T_{vjop} during continuous operation to 150°C from 125°C for the 6th-generation IGBT-IPM. This is due to the adoption of technologies that enable high temperature operation, such as high heat-resistant gel and highly reliable solder, which are 7th-generation packaging technologies. In addition, the maximum junction temperature T_{vjmax} has been expanded from 150°C to 175°C. This enables the size reduction of cooling parts in the equipment.

4. Contribution to the Size Reduction of Applied Equipment

This section describes a size reduction case study where a 60-mm width servo amplifier equipped with the P629 6th-generation IGBT-IPM can be made more compact using the P639 7th-generation IGBT-IPM. As shown in Fig. 11, there is a back-fin type servo amplifier, which has the cooling part attached in the rear of the casing. In this type of servo amplifier, the width of the servo amplifier casing can be reduced due to the reduced width of the short-side direction of the IGBT-IPM. That is, the replacement from the P629 to the P639 can reduce the amplifier width by 13.5 mm (approx. 20%). This means that the control panel containing the servo amplifier is made more compact, and as a result, it is expected to reduce the space of the entire servo systems.

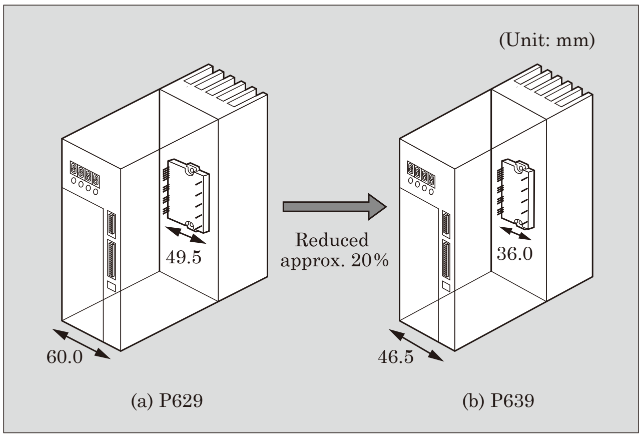

Fig.11 Schematic diagram of a back-fin type servo amplifier

5. Postscript

This paper described the features of the P639, which is the new compact series of 7th-generation IGBT-IPMs equipped with RC-IGBT chips.

Fuji Electric is confident that the expansion of this line-up of compact products will contribute to further reductions in the size of power conversion equipment.

In the future, we intend to continue advancing technological innovations and develop products to meet market demand. Furthermore, through the development of IGBT modules, Fuji Electric is committed to advancing measures against global warming to realize a safe and sustainable society.

References

(1) Minagawa, K. et al. 7th-Generation “X Series” IGBT-IPMs. FUJI ELECTRIC REVIEW. 2019, vol.65, no.4, p.210-214.

(2) Terashima, K. et al. 7th-Generation “X Series” IGBT-IPM with “P644” Compact Package. FUJI ELECTRIC REVIEW. 2020, vol.66, no.4, p.221-226.

(3) Minagawa, K. et al. “P631” Package 7th-Generation “X Series” High Power IGBT-IPM. FUJI ELECTRIC REVIEW. 2021, vol.65, no.4, p.247-251.

(4) Satou, K. et al. “The 7th Generation Intelligent Power Module for Industrial Applications”. Proceeding of PCIM Asia 2021.

(5) Ebukuro, Y. et al. 7th-Generation “X Series” RC-IGBT “Dual XT” Modules for Industrial Applications. FUJI ELECTRIC REVIEW. 2021, vol.67, no.4, p.242-246.

(6) Kawabata, J. et al. “The New High Power Density 7th Generation IGBT Module for Compact Power Conversion Systems”. Proceeding of PCIM Europe 2015.

3.3-kV 7th-Generation "X Series" IGBT Chip Technology

IKURA, Yoshihiro* HARADA, Yuichi* SEKINO, Yusuke*

ABSTRACT

The railways, including high-speed rails, use IGBT modules for drive motors. It is essential for IGBT modules to reduce power loss, as they directly contribute to CO_2 reduction. To meet this demand, Fuji Electric has developed a 3.3-kV SiC hybrid module that combines the latest generation "X Series" IGBTs and SiC-SBDs. Using a finer surface structure and a thinner drift layer, the X Series IGBT chip has reduced the collector-emitter saturation voltage by 1.0 V, compared with a previous generation. In addition, by combining it with a SiC-SBD, the hybrid module has achieved significant performance improvements with a turn-on loss reduction of 51% and reverse recovery loss reduction of 98%.

1. Introduction

Against the backdrop of global warming, various initiatives to reduce CO_2 emissions are underway. Approximately 20% of Japan's total CO_2 emissions come from transportation-related activities, and progress is being made in the electrification of transportation. In particular, high-speed rail emits far less CO_2 than airplanes, and for this reason, the number of new railways has increased in recent years, both in Japan and around the world.

Insulated gate bipolar transistor (IGBT) modules are used to drive motors for railway transportation. To reduce power consumption and reduce CO_2 emissions, power-loss reduction in IGBT modules is essential. In addition, to reduce the power consumed by high-speed rail itself, it is essential to reduce the weight of the rolling stock and onboard equipment, leading to demand for IGBT modules that can contribute to reductions in size and weight of the system are essential.

Conventional IGBT modules consist of Si-IGBTs and Si-PiN diodes made from silicon (Si). Practical application of silicon carbide (SiC), a next-generation power semiconductor material, has begun. The use of SiC can significantly reduce losses compared with silicon.[(1),(2)] As devices that use SiC, the introduction of Schottky barrier diodes (SBDs), which have a simpler device structure and manufacturing process, has advanced ahead of metal-oxide-semiconductor field-effect transistors (MOSFETs) and IGBTs.

Fuji Electric has developed a 3.3-kV-rated SiC hybrid high power module (HPM) that combines the latest generation "X Series" IGBT and the SiC-SBD to achieve significant loss reduction.[(3)] This paper describes the 3.3-kV X Series IGBT chip (X-IGBT) technology.

2. Features of 3.3-kV "X Series" IGBT Chips

2.1 Loss reduction technology

(1) Reduction of conduction loss

Figure 1 shows the cross section structures of an IGBT. IGBTs, in which electrons are injected from the MOS channel on the surface and holes are injected from the p^+ collector layer on the back in response, allow carriers (electrons and holes), which are particles responsible for the current, to accumulate in the n^- drift layer with low impurity concentration, resulting in low conductivity modulation to reduce conduction loss. Compared with the conventional "U Series" IGBT chips (U-IGBTs), the newly developed X-IGBT has a finer surface structure that enhances injection enhancement effect to increase the carrier density in the n^- drift layer, reducing the resistance of the n^- drift layer.

Furthermore, the use of advanced thin wafer tech-

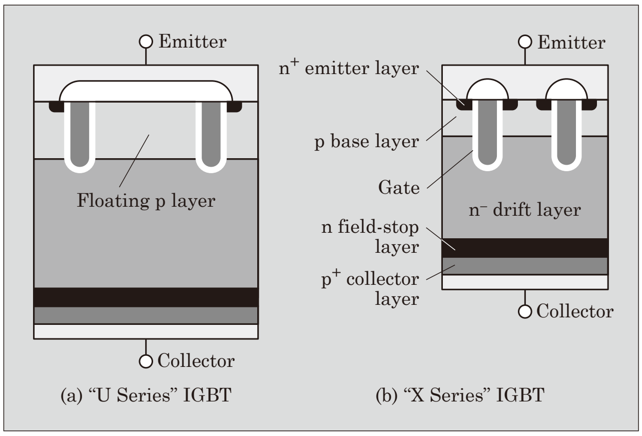

Fig.1 Cross section structures of IGBTs

* Semiconductors Business Group, Fuji Electric Co., Ltd.

nology has made the n⁻ drift layer thinner, thereby physically reducing the length of the conduction pathways of the current flowing between the collector and emitter electrodes, leading to a reduction in the resistance of the n⁻ drift layer.

Figure 2 shows the waveform of collector current I_C and collector-emitter voltage V_{CE}. By reducing the resistance of the n⁻ drift layer as described above, the X-IGBT has the lower V_{CE} than the conventional U-IGBT by 1.0 V at its rated current.

Figure 3 shows the relationship between the turn-off loss E_{off} and the collector-emitter saturation voltage $V_{CE(sat)}$. In general, there is an trade-off relationship between E_{off} and $V_{CE(sat)}$, where increasing a p⁺ collector layer concentration to reduce the $V_{CE(sat)}$ will increase the E_{off}. At the same E_{off}, the $V_{CE(sat)}$ has been lowered for X-IGBT than the conventional one by 1.0 V.

(2) Improved controllability of di/dt and dv/dt at turn-on

As shown in Fig. 1, a structure with a floating p-layer on the surface has been conventionally adopted to reduce the on-state voltage by suppressing the carrier emission and enhancing the injection enhancement effect. However, the presence of a floating p-layer increased the di/dt and dv/dt at turn-on, the suppression of which required higher gate resistance, resulting in an increase in turn-on loss E_{on}. The presence of a floating p-layer deteriorates the controllability of di/dt and dv/dt. As shown schematically in Fig. 4, it was revealed through cause analysis that holes accumulate in the floating p-layer, the potential of the floating p-layer increases rapidly, and the rate of increase in the potential (dv/dt) causes a displacement current to flow through the gate electrode, which leads to faster charging of the gate electrode regardless of the resistance value of the gate resistance R_G.[4]

As a result of the refinement of the surface structure, the X-IGBT achieves a low on-state voltage without using a floating p-layer, and the elimination of the floating p-layer improved the controllability of di/dt and dv/dt by R_G at turn-on. Figure 5 shows the di/dt R_G dependence at turn-on. When the R_G increases, the di/dt of the conventional product slightly decreases, whereas that of the X-IGBT largely decreases. For example, when di/dt is set to 0.15 kA/μs, the R_G needs to be 60 Ω or greater for the U-IGBT, but only approximately 40 Ω for the X-IGBT, allowing the E_{on} to reduce.

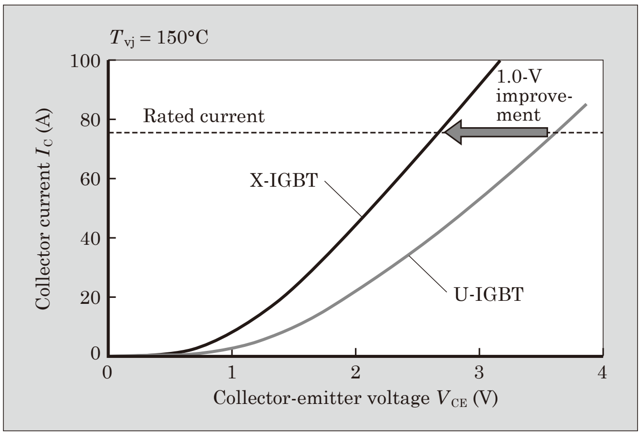

Fig.2 Collector current to collector-emitter voltage waveforms

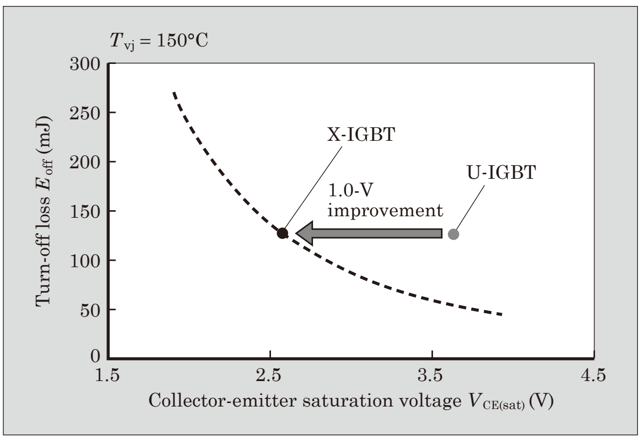

Fig.3 Relationship between the turn-off loss and the collector-emitter saturation voltage

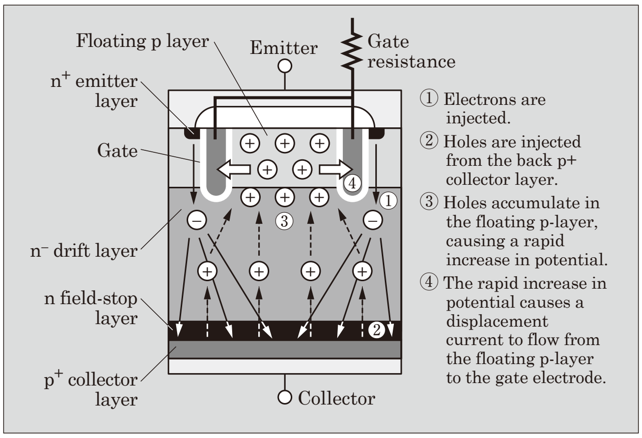

Fig.4. Floating p-layer and displacement current schematic diagram

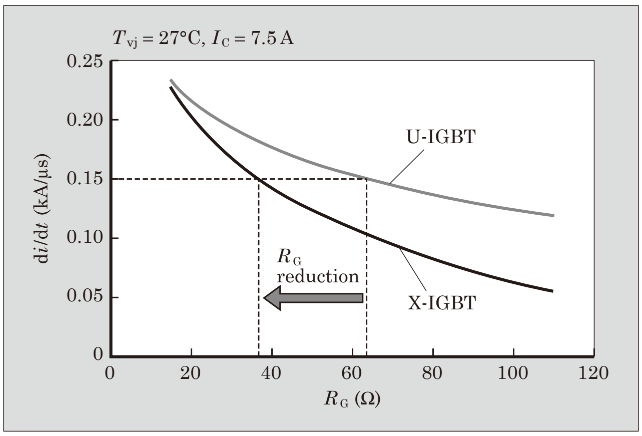

Fig.5 di/dt R_G dependence at turn-on

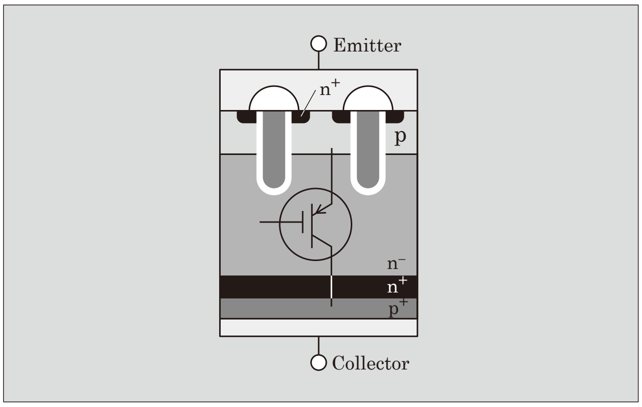

Fig.6 Parasitic PNP bipolar transistors in the IGBT

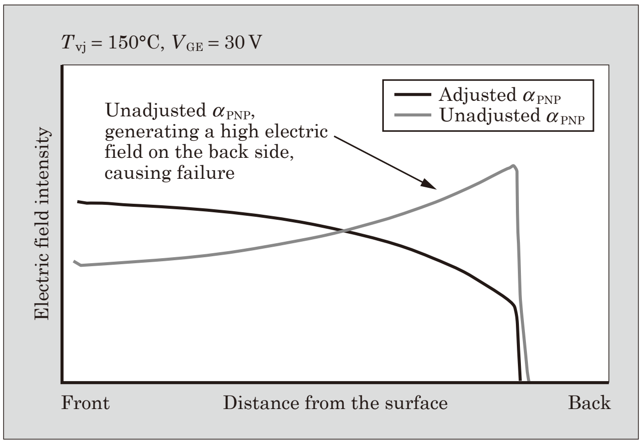

Fig.7 Electric field distribution during the short-circuit of the 3.3-kV IGBT

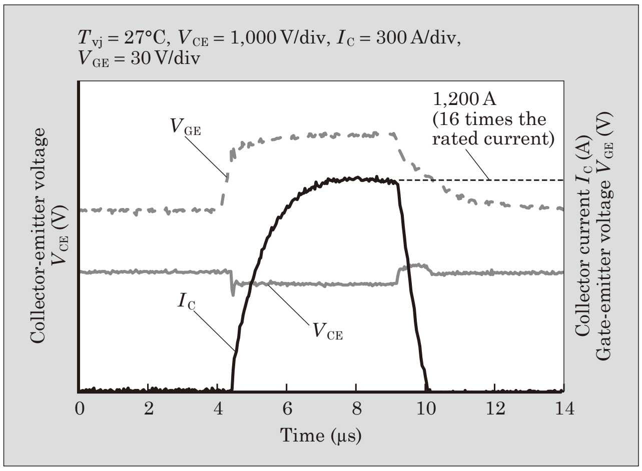

Fig.8 Waveforms during short-circuit operation

2.2 Technology for improving short-circuit ruggedness

IGBTs must have a short-circuit ruggedness to remain intact for a certain amount of time under short-circuit conditions. However, high blocking voltage IGBTs have less positive fixed charge in the n⁻ drift layer, which makes it easier for the positive fixed charge to be canceled out by the large number of electrons injected during the short circuit. As a result, the peak of the electric field shifts to the back side and causes avalanche breakdown, leading to IGBT breakdown (back side avalanche breakdown).[5]

To avoid this back side avalanche breakdown, it is effective to optimize the injection of holes from the back side. Optimizing hole injection from the back side is possible by controlling the gain of the parasitic PNP bipolar transistor in the IGBT shown in Fig. 6.

$$\alpha_{PNP} = \alpha \times \beta \times \gamma \quad \cdots\cdots (1)$$

α_{PNP}: Base ground current gain
α: Collector efficiency
β: Base transmission efficiency
γ: Emitter injection efficiency

Where α_{PNP} is the base ground current gain, α is the collector efficiency, β is the base transmission efficiency, and γ is the emitter injection efficiency.

According to Equation (1), the α_{PNP} is adjustable by β, which is determined by the neutral region of the n field-stop layer, and γ, which is determined by the p^+ collector layer. By optimizing layers such as the n field-stop layer and the collector layer, it is possible to control the injection of holes from the back side and bring α_{PNP} to an appropriate value. This adjustment can inhibit back side avalanche breakdown during the short-circuit period.

Figure 7 shows the electric field distribution of a 3.3-kV IGBT during the short-circuit. It suggests that adjusting the α_{PNP} to an appropriate value can suppress the increase of the electric field on the back side.

However, the n field-stop layer or collector layer that has been adjusted from the conventional one so that only the α_{PNP} is an appropriate value increases the leakage current at high temperatures, increasing the risk of failure during high-temperature operation. To overcome this issue, we use the newly developed n field-stop layer and collector layer for the X-IGBT. By optimizing the concentration distribution, this series has achieved an appropriate value of α_{PNP} while suppressing the leakage current. This optimizes hole injection during the short-circuit period to suppress the leakage current at high temperature operation while suppressing back side avalanche breakdown. Figure 8 shows waveforms during short-circuit operation. We have confirmed that the X-IGBT can turn-off a current 16 times the rated current without failure.

3. Application Example (Loss Reduction through Combination with SiC-SBDs)

In the newly developed 3.3 kV-rated SiC hybrid HPM, replacing a conventional Si-PiN diode to a newly developed SiC-SBD as the free wheeling diodes to be combined with an IGBT can not only reduce the reverse recovery loss E_{rr} of the diode, but also reduce the E_{on} of the IGBT.

The Si-PiN diode accumulates minority carriers inside the device when conducting, so that it needs to

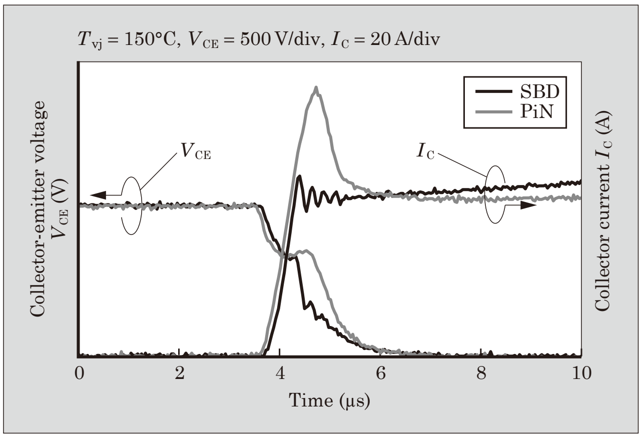

Fig.9 Turn-on waveforms

Table 1 Switching loss comparison

Item	Conventional HPM Si-PiN/Si-IGBT	New HPM SiC-SBD/ Si-IGBT	improve-ment rate
Turn-on loss (mJ)	2,933	1,425	51%
Turn-off loss (mJ)	1,957	1,900	3%
Reverse recovery loss (mJ)	1,548	30	98%

sweep out the carriers at turn-off time. This operation, appearing as the reverse recovery peak current I_{rp} in the reverse recovery waveform of the free wheeling diode, results in the superimposition on the collector peak current I_{cp} in the turn-on waveform of the IGBT, causing a corresponding loss. On the other hand, SiC-SBDs do not accumulate carriers inside the device, and therefore, I_{cp} and I_{rp} do not occur in principle, and no corresponding loss occurs. Figure 9 shows the turn-on waveforms of an IGBT combined with a Si-PiN diode and a SiC SBD. The combination with a Si-PiN diode produces a large I_{cp}, while the combination with a SiC-SBD produces no I_{cp}.

Table 1 shows a comparison of switching losses between the new product and conventional products.

Using a SiC-SBD reduced E_{on} and E_{rr} by 51% and 98%, respectively, achieving significant characteristic improvements.

4. Postscript

In this paper, we described the chip technology for the 3.3-kV latest generation “X Series” IGBT. This technology has improved losses by optimizing the surface and back structures. The 3.3-kV SiC hybrid high power module equipped with 3.3-kV X Series IGBTs described in this paper have been commercially used for high-speed rail. These modules have contributed to the reduction of power consumption of the high-speed rails as well as to reductions in the size and weight of equipment.(6) Moving forward, we will continue to improve the characteristics of IGBTs and contribute to the creation of a responsible and sustainable society by reducing CO_2.

References

(1) Takasaki, A. et al. “All SiC module with 1700 V rated 2nd generation trench gate SiC-MOSFETs”. International Exhibition and Conference for Power Electronics, Intelligent Motion, Renewable Energy and Energy Management (PCIM Europe), 2021.

(2) Sekino, Y. et al. “High Power next Core (HPnC) package with 3.3 kV SiC Hybrid chip combination”. International Exhibition and Conference for Power Electronics, Intelligent Motion, Renewable Energy and Energy Management (PCIM Asia), 2018.

(3) Sekino, Y. et al. 3.3-kV SiC Hybrid High Power Modules for Railcars. FUJI ELECTRIC REVIEW. 2021, vol.67, no.1, p.66-68.

(4) Onozawa, Y. et al. “Development of the next generation 1200 V trench-gate FS-IGBT featuring lower EMI noise and lower switching loss”. International Symposium on Power Semiconductor Devices and ICs (ISPSD), 2007.

(5) Onozawa, Y. et al. “Development of the next generation 1700 V trench-gate FS-IGBT” International Symposium on Power Semiconductor Devices and ICs (ISPSD), 2011.

(6) Fujita, K. et al. Power Electronics Equipment for Railcars Contributing to Safe, Secure, and Comfortable Public Transportation in the World. FUJI ELECTRIC REVIEW. 2021, vol.67, no.1, p.21-25.

“FA8C00 Series” 7th-Generation PWM Power Supply Control ICs

MATSUMOTO, Shinji* YAMANE, Hiroki* MIYAGI, Kodai*

ABSTRACT

The recent electronic equipment market has increasingly seen advances in energy. This trend has increased the demand for switching power supplies for electronic equipment with high efficiency in power conversion at light loads, high voltage AC input, and compactness. Fuji Electric has thus developed the “FA8C00 Series” 7th-generation PWM power supply control ICs. Minimum output pulse width is selectable for optimal MOSFET gate drive, improving power conversion efficiency at light loads. The maximum applied voltage at the high voltage AC input terminals has increased from 650 V to 710 V. Furthermore, clamping the IC output voltage eliminates the need for an external regulator circuit, reducing the number of components.

1. Introduction

As measures to address the critical issue of global warming, efforts to reduce greenhouse gas emissions have become extremely important. The growing concern about environmental problems has increased the demand for energy saving also in switching power supplies for electronic equipment. In particular, the expansion of network use and the increase of always-on systems in recent years have created a significant need to improve power conversion efficiency at light loads.

In emerging countries, the proliferation of electronic equipment progresses along with economic developments, meanwhile, voltage fluctuations in commercial power supplies (AC power supplies) are occurring frequently due to delays in infrastructure development. This causes high voltages exceeding the input voltage range of the power supplies, leading to power supply breakdown. On the other hand, the continued demand for lower prices for electronic equipment has also increased the need to reduce the size of power supplies and the number of components.

Fuji Electric has developed the “FA8C00 Series” of 7th-generation PWM power supply control ICs, which can further improve the power conversion efficiency of power supply systems at light loads, support high AC input voltages, and reduce the number of power supply components compared with the conventional product[1].

This paper provides an overview of the FA8C00 Series and describes its features as well as the effects of its application.

2. Product Overview

Figure 1 shows the external appearance of the FA8C00 Series. The FA8C00 Series use the same SOP-8, a compact package with 8 pins, as the conventional product did. This IC has a new function that allows external components to select the optimum minimum output pulse width for gate drive of metal-oxide-semiconductor field-effect transistors (MOSFETs) to improve power conversion efficiency at light loads.

The maximum applied voltage of the input ter-

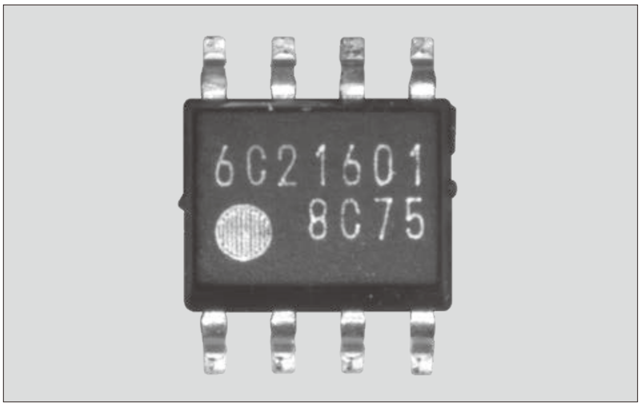

Fig.1 “FA8C00 Series” external appearance

Table 1 “FA8C00 Series” function overview

Item	Conventional products	FA8C00 Series
Minimum output pulse width selection function	Not provided	Available
Maximum applied voltage of the high AC input voltage terminal	650 V	710 V
IC output voltage clamp function	Not provided	Available (16 V)
External regulator	Required	Not required (8 components reducible)

* Semiconductors Business Group, Fuji Electric Co., Ltd.

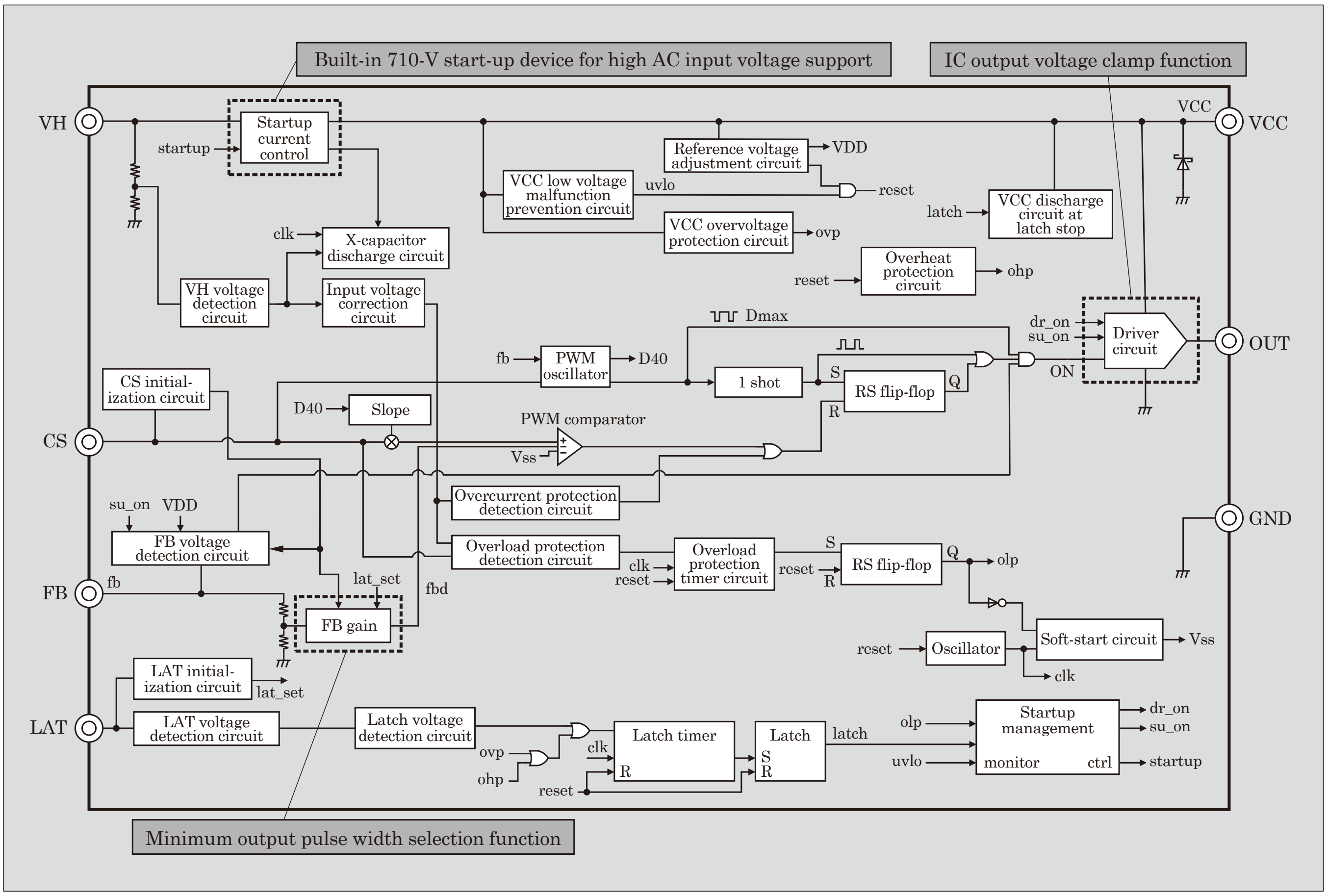

Fig.2 “FA8C00 Series” block diagram

minal connected to the AC power supply has also increased from 650 V to 710 V to prevent breakdowns caused by the application of high voltage from the AC power supply. Furthermore, to reduce the number of power supply components for this series, it uses an IC output voltage clamp function that prevents gate overvoltage breakdown of the MOSFET, eliminating the need for a conventional external regulator circuit.

Table 1 is an overview of the functions of the FA8C00 Series. Figure 2 shows a block diagram of the FA8C00 Series. The FA8C00 Series has an FB gain circuit to selects the minimum output pulse width, a startup current control circuit to support high AC input voltage with a built-in 710-V start-up device, and a driver circuit to clamp IC output voltage.

3. Features

3.1 Improved efficiency at light loads

To improve power conversion efficiency, as shown in Fig. 3, the conventional product performed a burst operation that continuously repeats the starting and stopping of switching operation to reduce switching loss. Figure 4 shows the relationship between the output pulse width of the OUT terminal and the voltages of the CS and FB terminals. The output pulse width of the OUT terminal for driving MOSFETs during continuous switching operation is determined by the comparison result of the current sense input (CS) terminal voltage V_{cs} and the voltage V_{fbd} obtained from the feedback control signal input (FB) terminal voltage divided inside the IC. However, narrow-width pulses generated due to the low voltages at the FB terminal when the switching operation starts and stops. This reduces the amount of power sent to the output side of the power supply in a single switching operation. As a result, the number of switching operations increases to compensate for the power shortage and, in turn, expands the switching loss, thus lowering the power

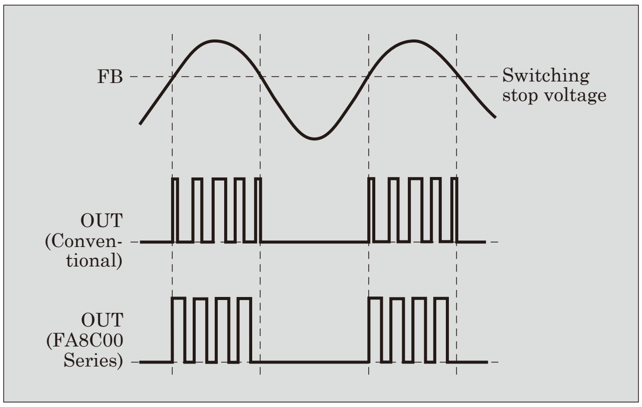

Fig.3 Burst operation

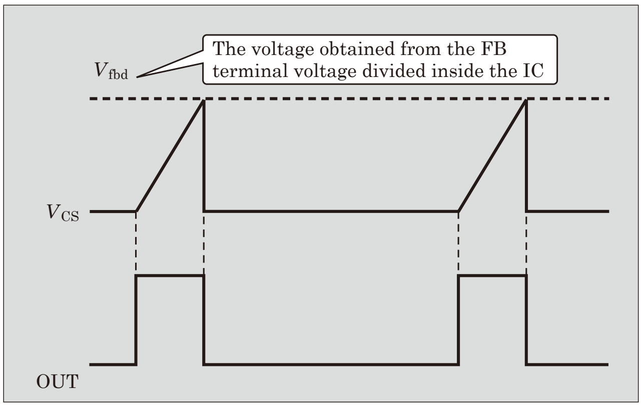

Fig.4 Relationship between the output pulse width of the OUT terminal and the voltages of the CS and FB terminals

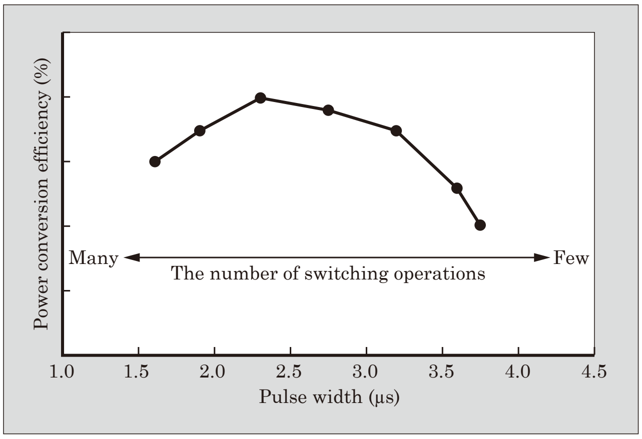

Fig.5 Power conversion efficiency variation with output pulse width

	High	Middle	Low
V_{fbd}	V_{fbd_h}	V_{fbd_m}	V_{fbd_l}
R1 ≤ 90 kΩ	C1 = 1,000 pF	C1 = 4,700 pF	C1 = 15,000 pF
R1 ≥ 200 kΩ	C1 = 1,800 pF	C1 = 3,300 pF	C1 = 6,800 pF

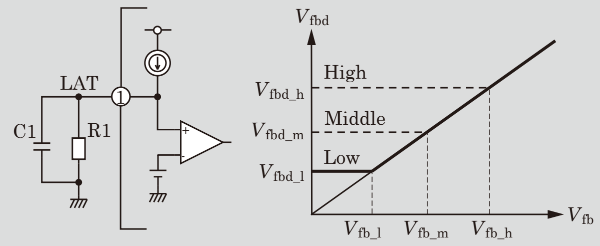

Fig.6 Selection of the minimum pulse width by an external component

conversion efficiency at light loads. On the other hand, as shown in Fig. 5, too wide-width pulses can reduce power conversion efficiency even if the number of switching operations is small, depending on the power supply, because the conduction loss of MOSFETs and diodes increase.

Consequently, optimizing the output pulse width is effective in improving the power conversion efficiency at light loads. For this reason, the FA8C00 Series has an additional function that allows an external component to set the minimum output pulse width according to the power supply. Figure 6 shows how the minimum pulse width is configured using an external component. The specific setting method is to connect a capacitor to the external latch signal input terminal (LAT terminal) and select the V_{fbd} voltage inside the IC, which determines the minimum output pulse width, by selecting the capacitance value of the capacitor C1 from one of the three capacities. As an example, assuming that R1 = 90 kΩ and C1 = 1,000 pF are connected, this function selects High to adjust the minimum output pulse width to be widest. This function enables the optimum minimum output pulse width to be set for each power supply, thereby improving the power conversion efficiency at light loads.

3.2 Increase in maximum allowable applied voltage for AC input

The internal circuit of the high AC input voltage terminal (VH terminal), which is connected to commercial power supplies (AC power supplies) and are required to have low power consumption, has a built-in junction field-effect transistor (JFET) as a start-up device. When starting up, the IC supplies a starting current (current for charging the VCC terminal at startup) from the VH terminal to the VCC terminal, which is the power supply of the IC, and stop the current when the VCC terminal voltage exceeds a certain voltage using the starting current control circuit. If more than the rated voltage of 650 V is applied to this start-up device, breakdown may occur.

The FA8C00 Series thus uses a start-up device modified to increase the maximum voltage applied to the VH terminal to 710 V to prevent breakdown under voltage fluctuations of commercial power supplies (AC power supplies).

3.3 Built-in output voltage clamp function

The FA8C00 Series has a built-in function to clamp the IC output voltage to prevent gate overvoltage breakdown of external MOSFETs. Figure 7 shows an external circuit configuration of the OUT terminal and an IC output voltage clamp circuit, and Fig. 8 shows IC output voltage clamp operations. For the existing FA8A80 Series, the VCC terminal voltage supplied from the auxiliary winding of the power supply can exceed a VCC terminal voltage of 30 V depending on the configuration of the power supply, and the MOSFET gate drive voltage output from the IC may also exceed 30 V. The typical rated voltage of a MOSFET gate is 20 to 30 V, and to prevent MOSFET breakdown, an external regulator circuit was previously required to ensure that the VCC terminal voltage is 20 V or less.

The new FA8C00 Series incorporates a function to clamp the IC output voltage inside the IC to keep

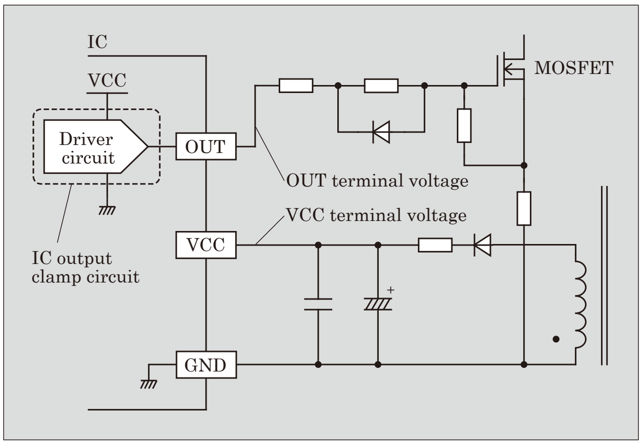

Fig.7 External circuit configuration of the OUT terminal and IC output voltage clamp circuit

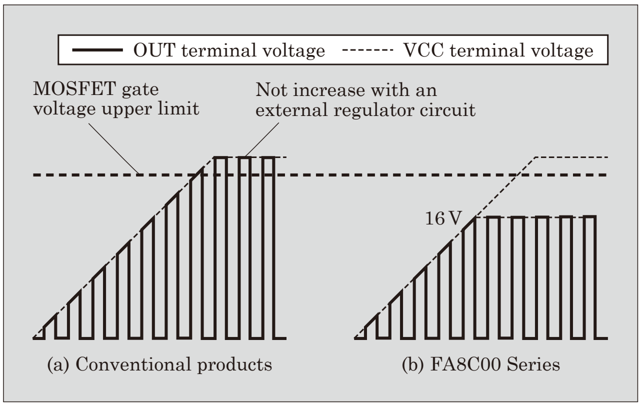

Fig.8 IC output voltage clamp operations

the gate voltage output from the IC to 16 V even if the VCC terminal voltage exceeds 30 V. This function eliminates the need for an external regulator circuit, thus reducing the number of power supply components.

4. Effects of Application to Power Circuits

4.1 Improved power conversion efficiency

Table 2 shows a comparison of power conversion efficiency with conventional product's, and Fig. 9 shows the measurement results of power conversion efficiency. In addition, Fig. 10 shows the circuit diagram of the FA8C00 Series power supply board for evaluation use, which was used for the measurement.

Table 2 Comparison of power conversion efficiency with conventional products

Products		Conventional products		FA8C00 Series	
Input voltage		115 V AC	230 V AC	115 V AC	230 V AC
Light load area power conversion efficiency	Output current 0.01 A	81.9%	78.2%	82.5%	79.7%
	Output current 0.02 A	85.7%	83.3%	86.6%	84.1%
	Output current 0.05 A	88.0%	86.8%	88.7%	87.2%
	Output current 0.1 A	89.0%	87.9%	89.5%	88.3%

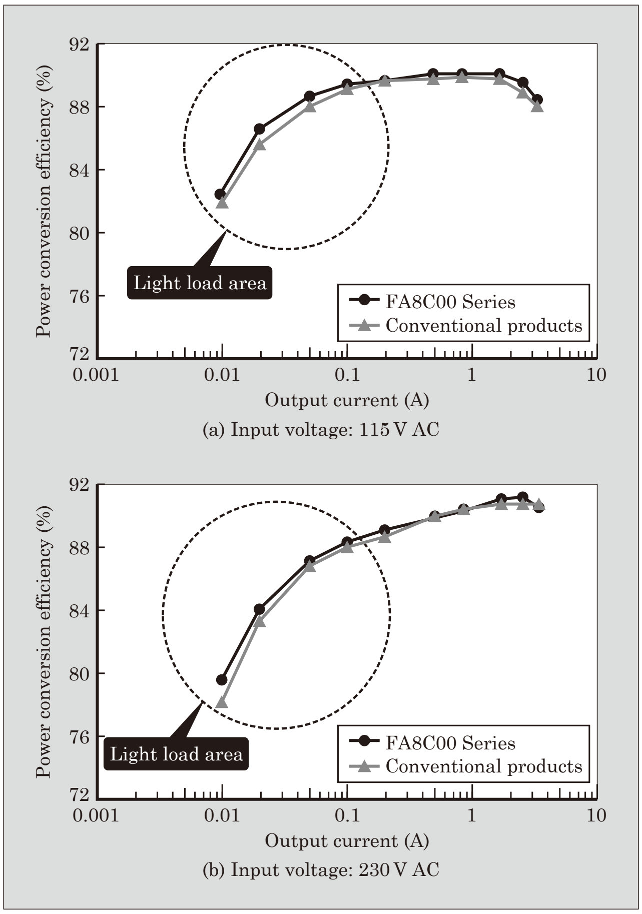

Fig.9 Power conversion efficiency measurement results

The results shows that the FA8C00 Series is more capable of improving the power conversion efficiency of light load ranges with a burst operation output current of 0.1 A or less than the conventional product. For instance, the efficiency has improved by +1.5% when the input voltage is 230 V AC and the output current is 0.01 A.

4.2 Reduction in the number of power circuit components

Figure 11 shows examples of the power supply circuits around the VCC terminal of the FA8C00 Series and the conventional product. Since the FA8C00 Series has a built-in clamp circuit in the IC as described above, even when the VCC terminal voltage is higher than the gate voltage of the MOSFET, it keeps the IC output voltage below the gate voltage of the MOSFET. This improvement eliminates the need for an external regulator circuit, which can reduce eight power supply components, contributing to a reduction in size of the power supply.

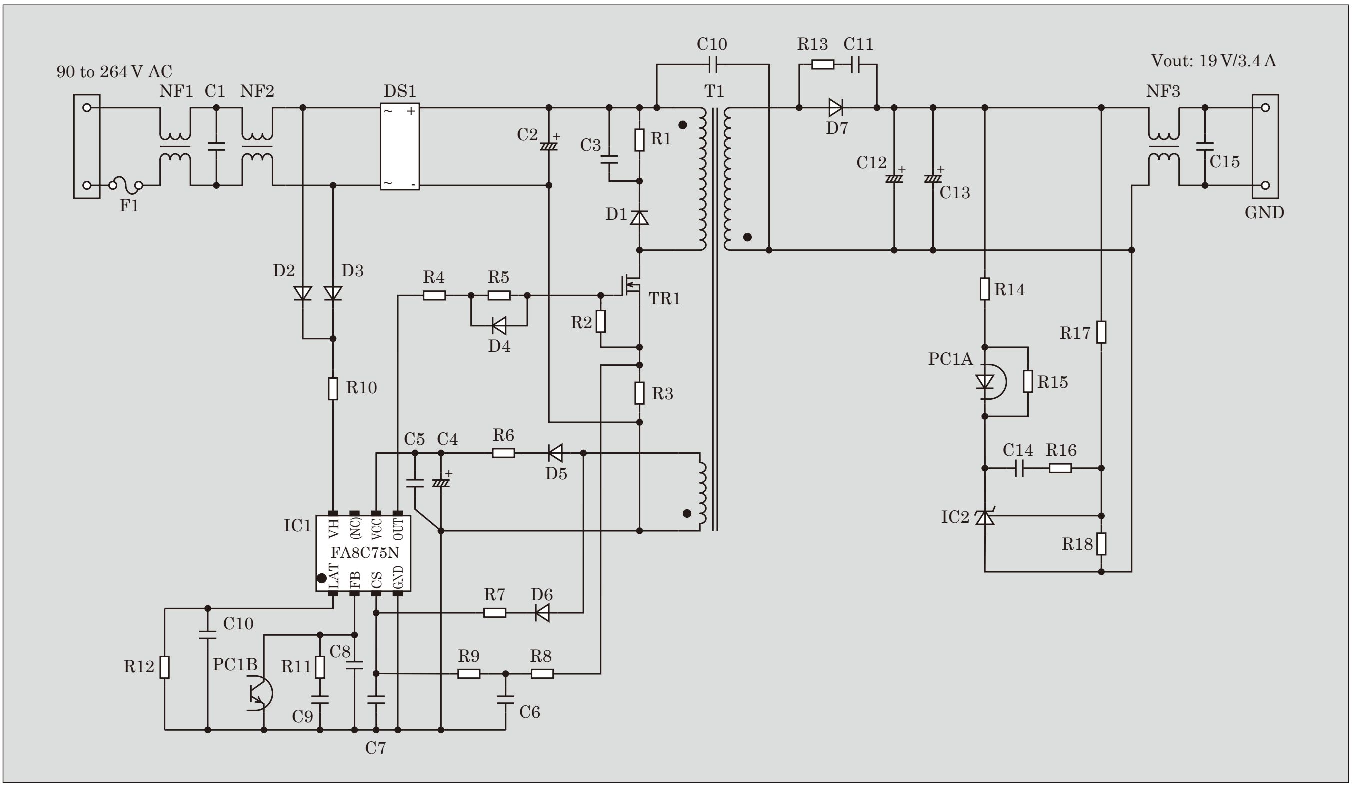

Fig.10 Circuit diagram of the power supply board for “FA8C00 Series” evaluation use (19 V/3.4 A, 65 W)

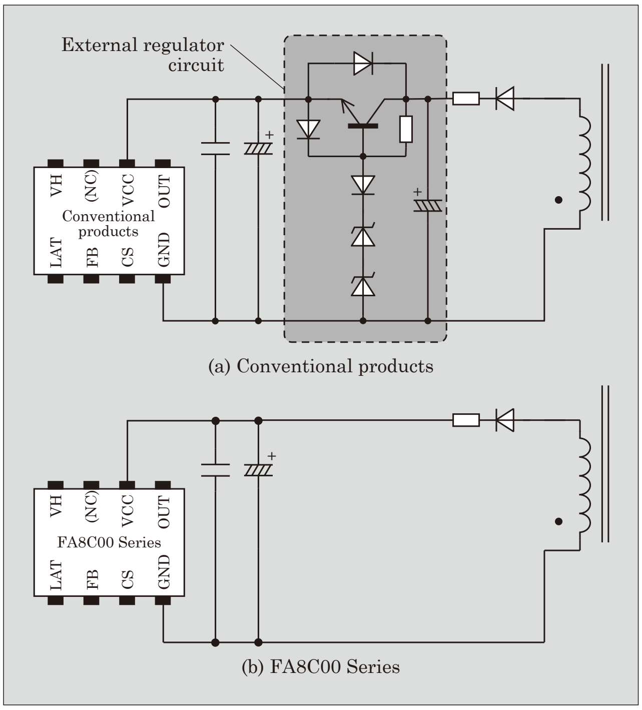

Fig 11 Examples of the power supply circuit around the VCC terminal of the “FA8C00 Series” and conventional products

5. Postscript

In this paper, we described the “FA8C00 Series” of 7th-generation PWM power supply control ICs. Current mode PWM power control ICs are required to have a variety of built-in functions to achieve a variety of power specifications.

Moving forward, Fuji Electric will continue to provide products that meet market needs of improving the power conversion efficiency at light loads and facilitating the reduction in the number of components to create compact power supplies.

References

(1) Hiasa, N. et al. “FA8A80 Series” 650-V PWM Power Supply Control ICs. FUJI ELECTRIC REVIEW. 2017, vol.63, no.4, p.237-241.

Auto-Zero Amplifier Technology for Intelligent Power Switches

IWAMOTO, Motomitsu*　TOYODA, Yoshiaki*　KATAKURA, Hideaki*

ABSTRACT

Electronic components installed in an automobile have recently increased in number and are therefore being required to be mounted with high density on the electronic control unit (ECU) board. They are also required to be miniaturized and integrated. Fuji Electric has therefore been studying the development of a next-generation intelligent power switch that integrates current drive devices, current-sensing amplifier, and a current detection shunt resistor into a single chip. Integrating a shunt resistor into the chip requires an amplifier with enhanced accuracy. We have thus developed a highly accurate auto-zero amplifier technology that automatically corrects output errors. This amplifier helps reduce the ECU board footprint while maintaining the same current detection accuracy as conventional products.

1. Introduction

In recent years, there has been strong demand for improved environment, safety, and comfort in automobiles. In terms of the environment, efforts are being made to improve the fuel efficiency and electrification of vehicles. In terms of safety, initiatives are being taken to promote autonomous driving, including advanced driver assistance systems. As for comfort, measures are being adopted to reduce the size of components to ensure larger interior space.

Fuji Electric has developed intelligent power switches (IPSs)[(1),(2)], pressure sensors[(3)], and igniters for automotive power ICs. IPSs are used as a current-drive device to drive solenoid valves for controlling transmissions. Reducing the size of IPSs and integrating peripheral components into a single chip enable miniaturization of the electronic control unit (ECU) board, which contributes to improved comfort by creating larger interior space. Improvement in the accuracy of IPS current detection also enables highly accurate control of the transmission, leading to high fuel efficiency.

Although miniaturization of the ECU board can be achieved by integrating the IPS and a shunt resistor for current detection into a single chip (instead of installing them separately), this increases the error of the current-sensing amplifier output and results in lower current detection accuracy. To solve this problem, we have developed an auto-zero amplifier technology that can prevent increase in output error even if the IPS and shunt resistor are integrated into a single chip. In this paper, we will provide an overview of the technology and describe some applications.

* Semiconductors Business Group, Fuji Electric Co., Ltd.

2. Challenges Related to Linear IPSs

2.1 Features of a linear IPS

IPSs are power ICs that add various control functions to power metal-oxide-semiconductor field-effect transistors (MOSFETs). Among the IPSs is a linear IPS that has a built-in amplifier that senses the current flowing into the load. Figure 1 shows the usage of Fuji Electric's conventional linear IPS.

A linear IPS supplies current to a load based on commands from a microcomputer. A shunt resistor converts the current into a voltage, which is then amplified by an amplifier and is fed back to an analog-digital converter (ADC) integrated into the microcomputer. The microcomputer adjusts its command value to the linear IPS in response to the feedback signal. This system allows accurate current to flow to the load (solenoid valve).

Fuji Electric's conventional linear IPS is a power IC that integrates a power MOSFET for current control, a control unit, and an amplifier for current detec-

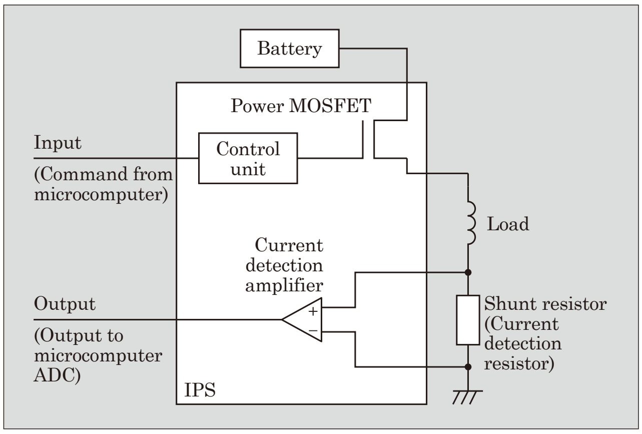

Fig.1 Conventional linear IPS usage

tion into a single chip as shown in Fig. 1, contributing to high-density mounting on ECU boards. To detect the current flowing through the load accurately, the current sensing amplifier has the circuit and layout design that is optimized to minimize the error generated in the output voltage.

2.2 Challenges related to single-chip integration

The greatest need for the linear IPS is to facilitate the miniaturization of ECU boards. Therefore, in order to achieve further miniaturization, we studied the integration of a shunt resistor in the linear IPS.

The biggest challenge when integrating shunt resistors is heat generation. If a resistor with the same resistance values as those of ECUs currently used in the market was incorporated in the chip, there would be a problem of excessive chip temperature rise due to Joule heat generated by the resistance. Considering the heat dissipation of the package, it is necessary to reduce the resistance value to one-fourth of the present value in order to integrate a shunt resistor into the chip. When the resistance is reduced to one-fourth, the input voltage of the amplifier is also reduced to one-fourth. Therefore, to maintain the input current-amplifier output voltage characteristic, the differential gain of the amplifier must be increased to 4 times the conventional gain (see Figs. 2 and 3).

By increasing the differential gain by a factor of 4, the input-output characteristic can be maintained, but at the same time, there is a disadvantage of increasing the error generated in the output voltage.

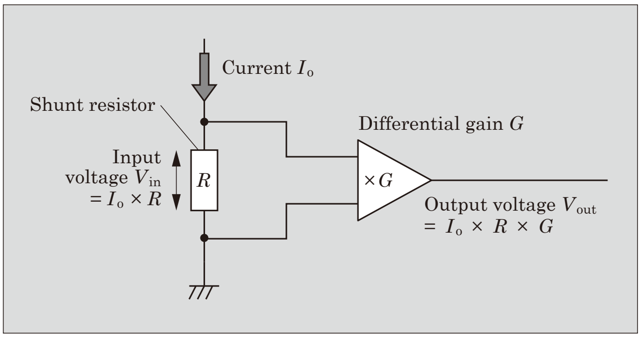

Fig.2 Shunt resistor and output voltage (conventional product)

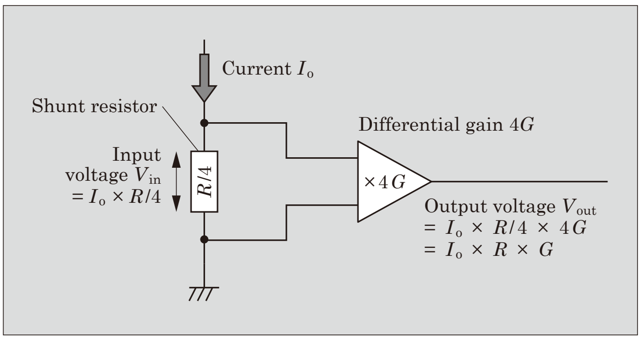

Fig.3 Shunt resistor and output voltage (newly developed product)

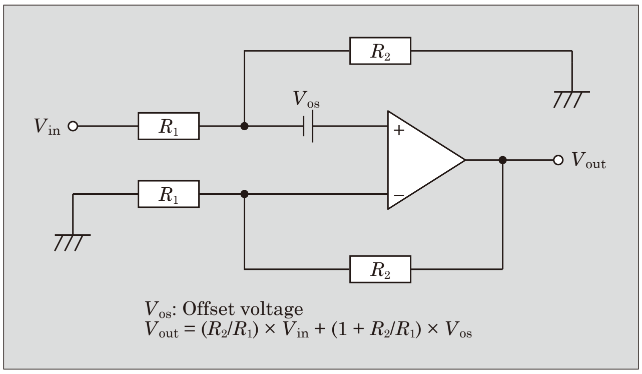

Fig.4 Differential amplifier circuit diagram

Figure 4 shows the circuit diagram of a differential amplifier using OP amplifiers with an offset voltage. The offset voltage is the error in the DC voltage generated at the input of the OP amplifiers. The error is caused by the difference between the threshold voltages of two paired transistors, called a differential pair, due to manufacturing variations. In the differential amplifier circuit shown in Fig. 4, denoting the input voltage as V_{in}, the output voltage as V_{out}, and the offset voltage as V_{os}, then the output voltage V_{out} is given by Equation (1).

$$V_{out} = (R_2/R_1) \times V_{in} + (1 + R_2/R_1) \times V_{os} \quad \cdots\cdots\cdots\cdots (1)$$

V_{in} : Input voltage
V_{out} : Output voltage
V_{os} : Offset voltage

Here, $(R_2/R_1) \times V_{in}$ is the magnitude of the signal and $(1 + R_2/R_1) \times V_{os}$ is the error due to offset voltage. Applying Equation (1) to Fig. 2, we obtain Equation (2), since R_2/R_1 corresponds to the differential gain G and V_{in} corresponds to the input current $I_o \times R$.

$$V_{out} = G \times I_o \times R + (1 + G) \times V_{os} \quad \cdots\cdots\cdots\cdots\cdots\cdots\cdots\cdots (2)$$

V_{out} : Output voltage
V_{os} : Offset voltage
G : Differential gain
I_o : Input current
R : Shunt resistor

On the other hand, in Fig. 3, the output voltage is expressed by Equation (3).

$$\begin{aligned} V_{out} &= 4\,G \times I_o \times R/4 + (1 + 4\,G) \times V_{os} \\ &= G \times I_o \times R + (1 + 4\,G) \times V_{os} \quad \cdots\cdots\cdots\cdots\cdots\cdots (3) \end{aligned}$$

Comparing Equations (2) and (3), the magnitude of the signal remains unchanged at $G \times I_o \times R$, while the error increases from $(1 + G) \times V_{os}$ to $(1 + 4\,G) \times V_{os}$. For example, if the differential gain G increases by a factor of 8, the error generated in the output voltage increases by a factor of approximately 4, from 9 V_{os} to 33 V_{os}.

Thus, integrating a shunt resistor allows the ECU board to be smaller but has the detrimental effect of increasing the error in the output voltage of the differential amplifier. To solve this problem, it is necessary to reduce the offset voltage of the OP amplifiers that comprise the differential amplifier.

Techniques to reduce the offset voltage include optimizing device layout on the chip and trimming during shipping tests. However, the effect of optimizing device layout is limited. In addition, it is difficult to compensate for offset voltage fluctuations due to temperature changes after adjustment when trimming during shipping tests. In light of this, we have developed and applied an auto-zero amplifier technology that self-compensates for offset voltages at regular intervals.

3. Features of Auto-Zero Amplifier Technology

3.1 Configuration of the next-generation IPS using an auto-zero amplifier

Figure 5 shows the block diagram of the next-generation IPS. As a countermeasure against the increase in error caused by an integrated shunt resistor, it uses an auto-zero amplifier as the current-sensing amplifier. Element devices include a power MOSFET for current drive, a control unit for controlling the power MOSFET, a shunt resistor, and a 5-V current-sensing amplifier (application of auto-zero amplifier), all on a single chip.

3.2 Auto-zero amplifier

(1) Operating principles

Figure 6 shows the operating principle of the auto-zero amplifier.

The auto-zero amplifier consists of two OP amplifiers, namely, a main amplifier and a correction amplifier. Each OP amplifier has an input terminal for offset voltage correction (CO terminals in the figure) in addition to the normal + and − inputs. $V_{os}1$ is the offset voltage of the main amplifier, and $V_{os}2$ is the offset voltage of the correction amplifier.

SW1 and SW2 alternately turn on and off, and SW3 and SW4 also alternately turn on and off. As for the timing of switching, SW1 and SW3 turn on simul-

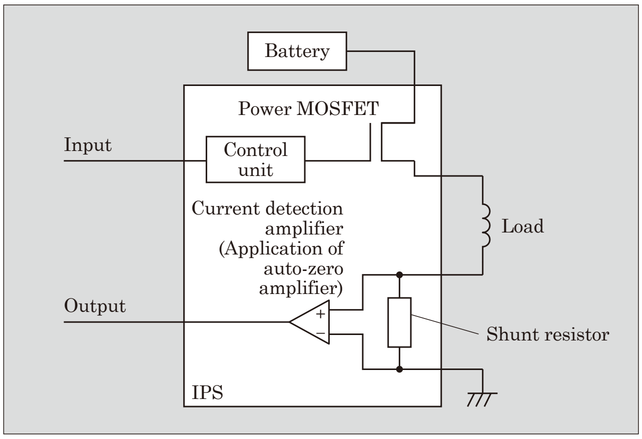

Fig.5 Block diagram of the next-generation IPS

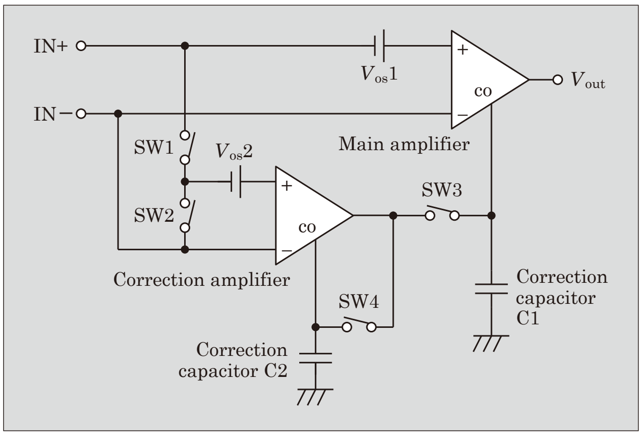

Fig.6 Operating principle of the auto-zero amplifier

taneously and SW2 and SW4 turn on simultaneously. Capacitors C1 and C2 hold the respective correction voltages of the main amplifier and correction amplifier.

The auto-zero amplifier operation is divided into two phases depending on the SW connection status.

(a) Phase 1: SW1 and SW3 = Off; SW2 and SW4 = On

A correction amplifier corrects its own offset voltage. Since both inputs of the correction amplifier are short-circuited, the correction amplifier receives its own offset voltage $V_{os}2$. The output of the correction amplifier is connected to its own correction terminal CO via SW4. Therefore, the correction amplifier outputs a voltage that cancels its own offset voltage $V_{os}2$ and charges the correction capacitor C2.

(b) Phase 2: SW1 and SW3 = On; SW2 and SW4 = Off

Correction is performed for the main amplifier. IN+ is connected to the + terminal of the correction amplifier via its own offset voltage $V_{os}2$, and IN− is connected to the − terminal. $V_{os}2$ is connected to the + terminal of the correction amplifier, but the correction amplifier has already been offset corrected in Phase 1 and no offset voltage component is superimposed on the output.

Since the main amplifier operates with negative feedback, the potentials of the main amplifier's + and − terminals become equal. Therefore, the voltage difference between IN+ and IN− becomes the offset voltage $V_{os}1$ of the main amplifier. The offset voltage $V_{os}1$ of the main amplifier is input to the correction amplifier. The correction amplifier outputs a voltage that cancels the offset voltage $V_{os}1$ of the main amplifier and charges the correction voltage to the correction capacitor C1 of the main amplifier.

By periodically repeating Phases 1 and 2, the correction voltages of the correction amplifier and main amplifier are always kept at the optimum value, minimizing the error generated by the main amplifier output.

(2) Reduction of operating power supply voltage

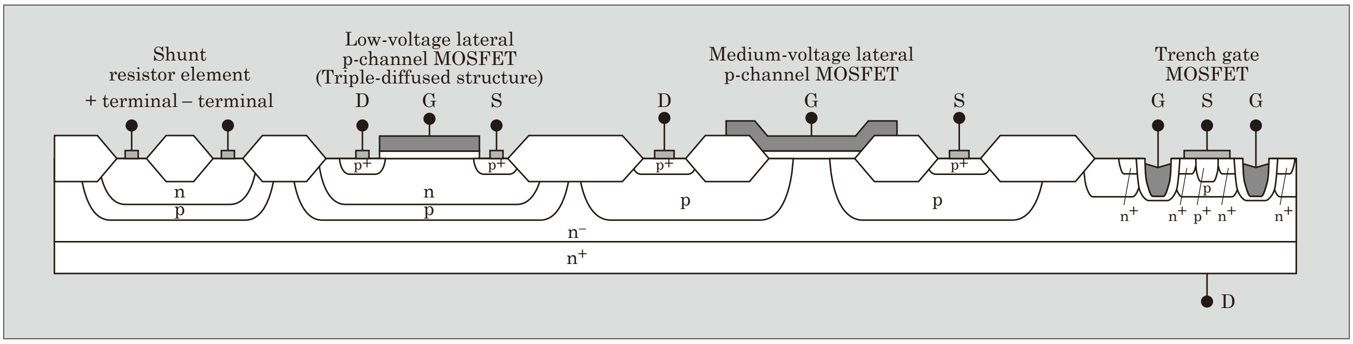

Fig.7 Cross-sectional structure of the 5th-generation IPS device

The next-generation IPS is required to integrate the power MOSFET with 5-V circuit on a single chip, and we have developed the auto-zero amplifier technology using 5th-generation IPS device and processing technology.[5] Figure 7 shows the cross-sectional structure of a device applying the 5th-generation IPS device processing technology. The feature of this process is that a trench gate MOSFET for current drive, a medium-voltage MOSFET, a low-voltage MOSFET with triple-diffused structure, and a shunt resistor can be integrated on a single chip. This makes it possible to achieve auto-zero amplifier technology that automatically corrects the offset voltage while providing the current drive capability and breakdown voltage performance required for automotive power ICs.

In general, a triple-diffused structure requires a high impurity concentration in the topmost layer, and MOSFETs formed in that layer tend to have a high threshold voltage. The same trend was observed for the low-voltage MOSFETs with a triple-diffused structure used in this research. Circuits composed of high-threshold-voltage MOSFETs will have a higher operable power supply voltage. In contrast, the market is requiring power supplies to operate at low voltages to improve tolerance to power supply voltage fluctuations. Therefore, we took the following measures to reduce the operating voltage in our newly designed auto-zero amplifier.

(a) Bias circuit

We have modified the bias circuit, which must start operating at the lowest power supply voltage of the circuits. In particular, we achieved low-voltage operation by changing the circuit configuration in areas with a large number of MOSFET layers and optimizing the bias conditions of the MOSFETs.

(b) Under voltage lockout (UVLO) circuit

The amplifier output becomes undefined when the power supply voltage is low and the operating voltage of the amplifier is not sufficient. Since outputting a signal to the microcomputer's ADC in an undefined state can cause a system malfunction, it is equipped with a UVLO circuit that fixes the amplifier output at 0 V until the amplifier output converges. If the reference voltage that fixes the amplifier at 0 V fluctuates due to manufacturing variations, the guaranteed operating voltage will be higher. Therefore, we have improved the circuit to minimize the effect of manufacturing variations on the reference voltage.

This innovation has made it possible to achieve an operating voltage equivalent to that of conventional products using a triple-diffused structure process.

4. Effect of the Auto-Zero Amplifier

Figure 8 shows the evaluation results of an actual device using an auto-zero amplifier. The gain was set to 32 times, four times that of the conventional product, taking into account that the shunt resistance is one-fourth of the conventional resistance. A load current applied to the input of the amplifier was 1 A and the voltage, equivalent to that when using one-fourth of the shunt resistance used for the conventional product. Current detection accuracy was evaluated under these conditions in a temperature range of −40°C to +175°C. The target value was equal to that of the 5th-generation IPS[4].

As shown in Fig. 8, the target specifications of the 5th-generation IPS are satisfied even though the gain is 32 times, which is four times that of the conventional product.

The evaluation results suggest the auto-zero am-

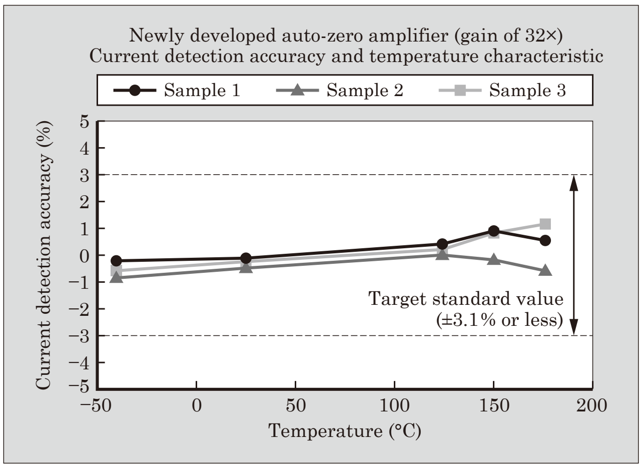

Fig.8 Evaluation results of an actual device using an auto-zero amplifier

plifier technology can solve the increase in error that would otherwise occur when an IPS and shunt resistor are integrated into a single chip. The built-in shunt resistor is expected to reduce the size of the ECU board, and the current detection accuracy is expected to be the same as that of conventional products.

5. Postscript

We have developed an auto-zero amplifier technology for IPSs that can be utilized in automotive power ICs. This is expected to reduce the size of the ECU board while maintaining the same level of current detection accuracy as conventional products.

In the automotive field, which is rapidly becoming more electronic, we believe that this technology will be used in a wide range of applications other than IPSs. Going forward, Fuji Electric continues to study ways to expand the scope of application and contribute to the automotive industry.

References

(1) Nakagawa, S. et al. One-Chip Linear Control IPS, “F5106H”. FUJI ELECTRIC REVIEW. 2013, vol.59, no.4, p.251-254.

(2) Toyoda, Y. “60 V-Class Power IC Technology for an Intelligent Power Switch with an Integrated Trench MOSFET”. ISPSD. p.147-150, 2013.

(3) Ashino, K. et al. 7th–Generation Automotive High-Pressure Sensors. FUJI ELECTRIC REVIEW. 2019, vol.65, no.4, p.249-253.

(4) Iwata, H. et al. “F5202H” 5th-Generation Intelligent Power Switch for Automotive Applications. FUJI ELECTRIC REVIEW. 2020, vol.66, no.4, p.206-210.

Trench SBD-Integrated SiC-MOSFET To Suppress Bipolar Degradation

BABA, Masakazu* TAWARA, Takeshi‡ TAKENAKA, Kensuke‡

ABSTRACT

When the body diode of a SiC-MOSFET is forward biased, characteristic degradation occurs as on-voltage increases with stacking faults expanding within the drift layer. To avoid the issue, integrating a trench SBD into a conventional SiC trench gate MOSFET will suppress a body diode current under forward bias without the need for increased chip size. This structure has increased the current density at which characteristic degradation occurs by approximately four times compared with conventional SiC trench gate MOSFETs. Without using external SBDs, this technology is expected to reduce the size and weight of products and reduce characteristic degradation, improving long-term reliability.

1. Introduction

In recent years, there has been growing demand for low-loss power conversion equipment to help achieve a decarbonized society. Compared with silicon (Si), silicon carbide (SiC) has a wider band gap and a higher breakdown electric field. Therefore, it has enabled to reduce resistance of the drift layer due to a thin and high carrier concentration. In addition, its high thermal conductivity and wide band gap allow the device to operate at high temperatures, thus streamlining the cooling system and benefiting power conversion equipment through size and weight saving. For example, in electric vehicles, the use of SiC power semiconductor devices enables inverters to be smaller and lighter and also extends the driving range by reducing losses. Power conversion equipment such as inverters use metal-oxide-semiconductor field-effect transistors (MOSFETs) and Schottky barrier diodes (SBDs). There is a known way to reduce the size of inverter circuits is to reduce the number of devices by using parasitic pn diode (body diode) in the MOSFET instead of external SBD as a free wheeling diode. However, the current flowing through the body diode of the SiC-MOSFET can increase losses due to the on-state voltage increase (bipolar degradation).

This paper will describe the suppression of bipolar degradation in SiC-MOSFETs through the integration with a trench SBD.

* Semiconductors Business Group, Fuji Electric Co., Ltd.
‡ The National Institute of Advanced Industrial Science and Technology (seconded from Fuji Electric)

2. Bipolar Degradation and Integrated SBD Suppression Effect

Figure 1 shows the cross sectional viewing of a SiC trench gate MOSFET device. It has been reported that when the current flows through the body diode formed around the trench gate, the forward voltage V_F and the voltage V_{on} at the start of operation, which are applied between the drain and source of the MOSFET, increase due to bipolar degradation.(1) Bipolar degradation is caused by a stacking fault (SF) expanding and forming a high-resistance layer under forward current stress. When the body diode is activated, electrons are injected from the drain side and holes are injected from the source side into the drift layer and substrate. The energy released by the recombination of injected electrons and holes causes the SFs to expand starting from the basal plane dislocation (BPD) present in the drift layer and substrate.(2)

The BPD is a dislocation defect that exists in SiC substrate. It is converted to a threading edge dislocation (TED) at the interface between the drift layer and

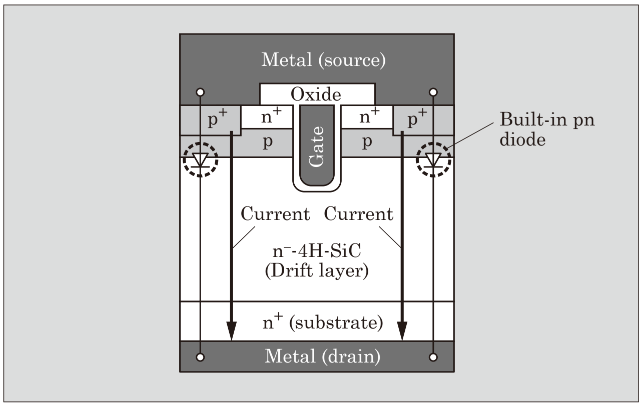

Fig.1 Cross section of a SiC trench gate MOSFET device

the substrate at the start of the epitaxial growth of the drift layer. A SF extends from the BPDs that penetrate the drift layer without being converted to a TED. SFs reportedly extend also from BPDs that has been converted to TEDs under a high current.[3]

Figure 2 shows the graph of ΔV_F versus forward current density up to 500 A/cm^2 in a conventional SiC trench gate MOSFET, where ΔV_F is a variation from the initial V_F, a voltage before the current stress. With no measures in place, ΔV_F increased when forward current was applied at a current density of 500 A/cm^2, showing bipolar degradation occurred.

Fuji Electric has developed a recombination promoting layer as a technology to suppress bipolar degradation. In the recombination promoting layer, which is a high carrier concentration layer formed between the drift layer and the substrate, minority carrier holes exhibit short carrier lifetime. Therefore, the number of holes injected from the drift layer into the substrate decreases, suppressing the expansion of SFs. In the future, power devices are expected to become smaller in chip size. To use them at higher current densities, their recombination promoting layer will need to be optimized for highly concentrated and thick film. In addition, we considered it effective not to activate the body diode and not to recombine electrons and holes as an alternative means of suppressing bipolar degradation. As a method to suppress bipolar degradation, this paper studies to integrate SBDs and MOSFETs into one chip (trench SBDs are incorporated).

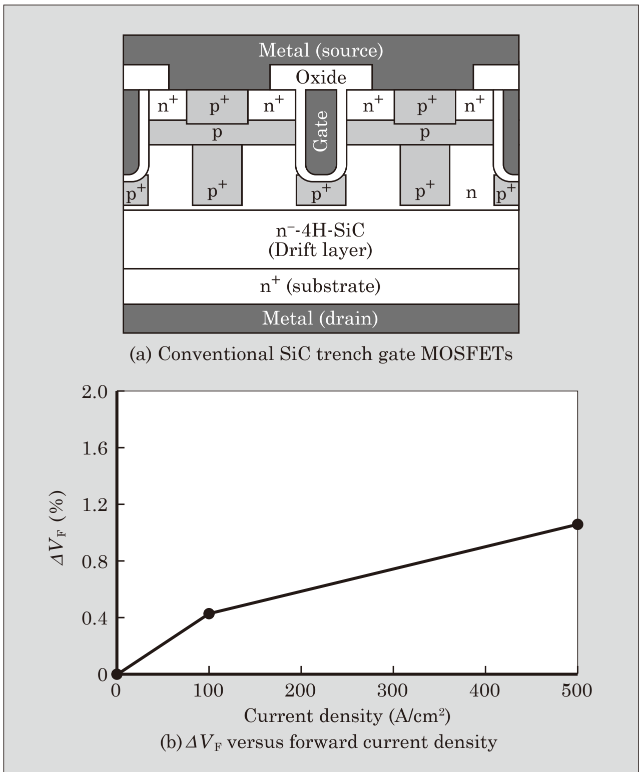

Fig.2 Conventional SiC trench gate MOSFET and bipolar degradation

Next, we will describe the principle of bipolar degradation suppression using an integrated trench SBD. Figure 3 shows the cross-sectional structure of the SiC trench gate MOSFET and the equivalent circuit when activating the body diode. The p-type layer under the SiC trench gate MOSFET and the trench SBD are each connected to the source through the surface p-type contacts in the depth direction (not shown in the figure). The equivalent circuit in Fig. 3 shows the current pathway when the body diode is activated. In contrast to the SiC trench gate MOSFET in Fig. 3(a), the SiC trench gate MOSFET with an integrated trench SBD (SBD-integrated MOSFET) in Fig. 3(b) has a trench SBD and built-in pn diode connected in parallel to share the resistance of drift layer. Although the parallel connection results in equal voltages applied to the trench SBD and the built-in pn diode, the trench SBD is actually formed at a far from the branch point in Fig. 3(b) than the built-in pn diode. We must thus take into account of the resistance between the SBD and the drift layer (spreading resistance). The voltage V_{pn} applied to the built-in pn diode shown in Fig. 3(b) is equal to the sum of the voltage V_{SBH} applied to the SBD and the voltage V_{sp} applied to the spreading resistance. Therefore, if the sum of V_{SBH} and V_{sp} is lower than the built-in voltage V_D of the built-in pn diode, the built-in pn diode will not turn on. V_{SBH} is generally deter-

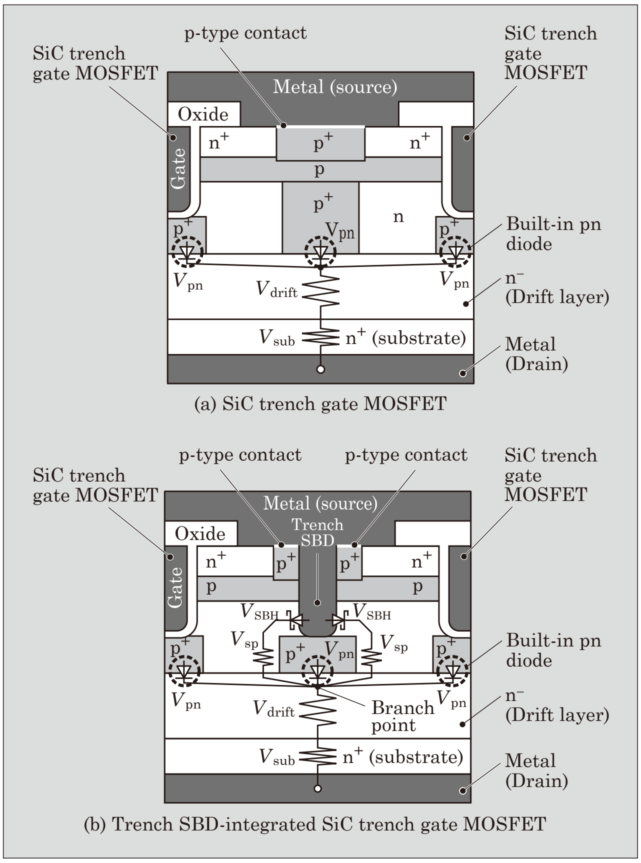

Fig.3 The cross-sectional structure of the SiC trench gate MOSFET and the equivalent circuit when the body diode is activated

mined by the potential barrier height at the Schottky junction and is smaller than V_D. Therefore, adjusting the V_{sp} suppresses the activation of the built-in pn diode. Instead of the built-in pn diode, the trench SBD, a unipolar device, is activated but does not cause bipolar degradation.

3. Characteristics of SiC-MOSFETs with Integrated Trench SBDs

We have established a technology and developed a prototype to form a trench SBD in a SiC trench gate MOSFET by participating in a research project of the joint research body Tsukuba Power-Electronics Constellations (TPEC). For the integration of a trench SBD, forming a planar SBD in conventional SiC trench gate MOSFETs, which have narrow cell pitch, causes wider cell pitch and increases V_{on}, resulting in higher loss. To avoid widening the cell pitch, we formed trench SBDs.

Figure 4 shows a cross-sectional scanning electron microscopy (SEM) image of a prototyped 1,200-V SiC trench gate MOSFET with an integrated trench SBD. We confirmed that a trench SBD was formed between the trench gates of the SiC trench gate MOSFET.

Figure 5 shows the breakdown voltage and current waveforms of a conventional SiC trench gate MOSFET and an SBD-integrated MOSFET at room temperature. It shows that both structures had break down voltage of over 1,200 V. There was no significant difference in the leakage current between the drain and the source, and we confirmed that the leakage current was not affected by the SBD-integrated MOSFET. Figure 6 shows the trade-off between specific on-resistance $R_{on} \cdot A$ and threshold voltage V_{th} at room temperature for a SiC trench gate MOSFET and SBD-integrated MOSFET with the same cell pitch. The gate structure, cell pitch, and active region size remain the same for both structures, resulting in almost identical characteristics.

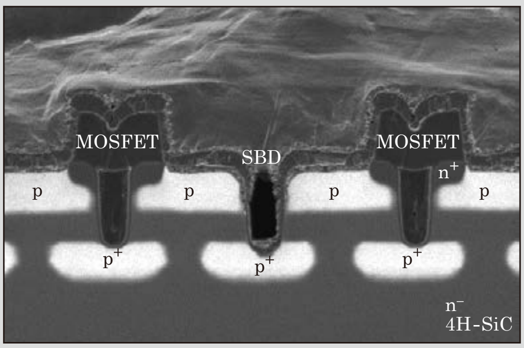

Fig.4 Cross-sectional SEM image of Trench SBD-integrated SiC trench gate MOSFET

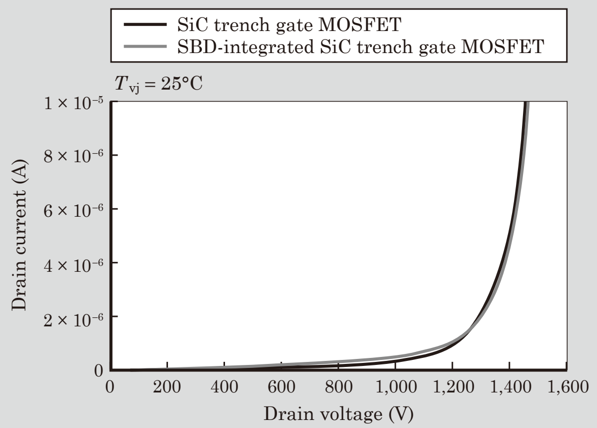

Fig.5 Breakdown voltage and current waveforms

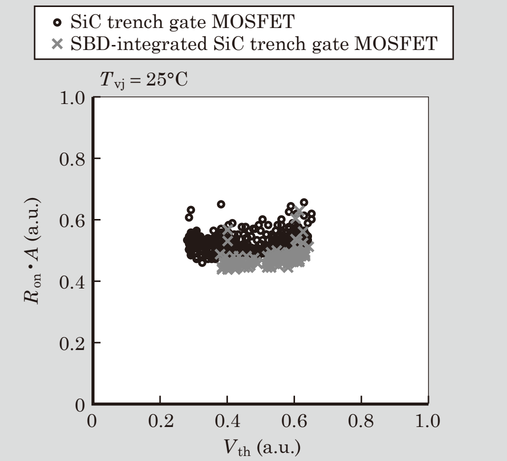

Fig.6 $R_{on} \cdot A$ - V_{th} trade-off

4. Verification of the Bipolar Degradation Suppression Effect

Figure 7 shows the J-V characteristics of the body diode at 150°C for a conventional SiC trench gate MOSFET and three types of SBD-integrated MOSFETs with different cell pitches. The cell pitch becomes narrower in the order of device A, device B, and device C.

First, for the conventional SiC trench gate MOSFET, when the built-in pn diode operates, bipolar currents, which consists of electron current and hole current, flows, resulting in exponentially increasing as shown in Fig. 7(a). In contrast, Figs. 7(b), 7(c), and 7(d) show linear characteristics at the initial increase of the J-V waveform. We suppose that V_{SBH} is smaller than the built-in voltage of the built-in pn diode, which activates only the SBD alone, resulting in only unipolar current, namely electron current. For devices A, B, and C, the current density tended to increase steeply as the applied voltage increased. It is thought that the built-in pn diode began to operate, following the trench

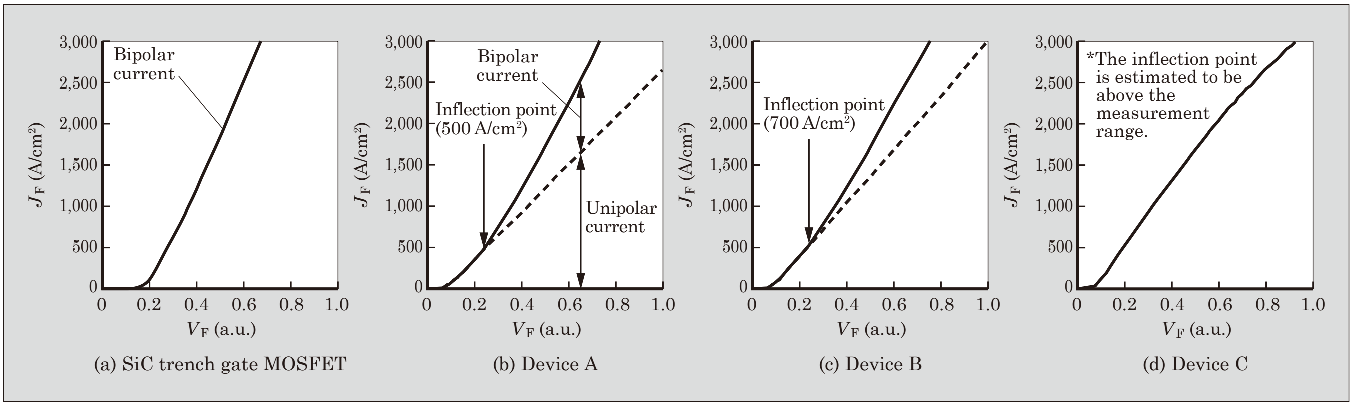

Fig.7 *J*-*V* characteristics of body diode at 150°C

SBD, at the boundary of the condition (inflection point) where the slope of the current increase changes rapidly. The current density at the inflection point tends to increase as the cell pitch becomes narrower. As the cell pitch narrows, the distance between the branch point in Fig. 3(b) and the SBD becomes shorter, the spreading resistance decreases, and V_{sp} decreases. As a result, it is assumed that the built-in pn diode became difficult to turn on. From the characteristics in Fig. 7(d), it is estimated that bipolar degradation does not occur in device C, which has the narrowest cell pitch, at a current density of 3,000 A/cm² or higher, which is six times higher than that at which bipolar degradation occurs in a conventional SiC trench gate MOSFET.

Next, we conducted a forward current stress test on the SBD-integrated MOSFETs to verify the suppression effect of bipolar degradation. We tested device B and device C to verify the effect before and after the inflection point and to verify whether bipolar degradation occurred at a current density of up to 2,000 A/cm², which is the highest value of the testing equipment. First, we heated device B to 150°C, which is the assumed operating temperature, and applied pulse current with an adjusted duty ratio to suppress the heat generation. After measuring the initial characteristics, we applied current to the devices at 300 A/cm², 700 A/cm², 1,000 A/cm², 1,500 A/m², and 2,000 A/cm². The effective conduction time was 5 minutes for up to 1,000 A/cm² and 2 minutes for 2,000 A/cm². We measured V_F again after forward current stress test and evaluated ΔV_F.

Figure 8 shows ΔV_F versus applied forward current density. We confirmed that there was no increase in ΔV_F under current density lower than 700 A/cm² at the inflection point. At current densities above 1,000 A/cm², we confirmed that ΔV_F increased and the characteristics degraded. Since the bipolar current component increases as the current density increases under conditions above the inflection point, the number of electrons and holes injected into the drift layer increases, leading to bipolar degradation. To check the degraded device for the presence of SFs, we peeled off its surface electrode to perform photo luminescence (PL) imaging measurement at a wavelength of 420 nm, where SFs emit light. Figure 9 shows the PL image of the device with increased ΔV_F after forward current stress. The area shown in white in Fig. 9 corresponds to the expanded SFs. Based on these results, we confirmed that bipolar degradation does not occur near the inflection point where the bipolar current component is small and at current densities lower than the inflection point because either the amount of electron and hole injection into the drift layer is small or the built-in pn

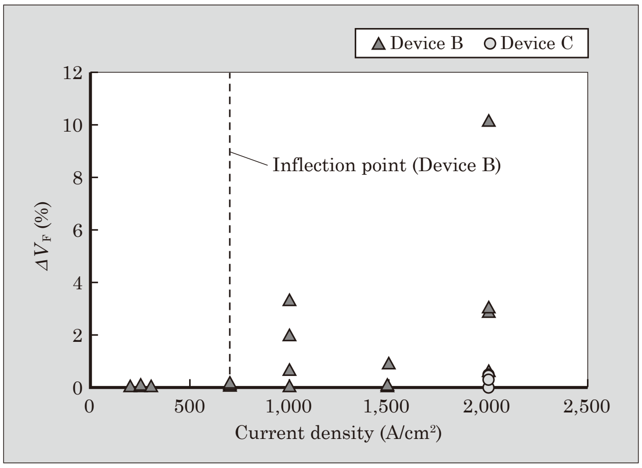

Fig.8 ΔV_F versus forward current density

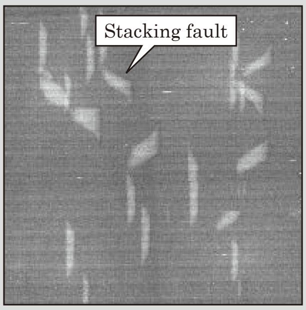

Fig.9 PL image of device with increased ΔV_F after forward current stress

diode does not operate.

After this, we conducted a forward bias stress test on device C, which exhibited an inflection point of higher current density. From the J-V waveform in Fig. 7(d), it can be inferred that ΔV_F does not fluctuate even at a current density of 2,000 A/cm^2. We then conducted a test on device C with an effective conduction time of 2 minutes at 175°C and 2,000 A/cm^2, the most severe conditions of the testing equipment. As shown in Fig. 8, device C showed no bipolar degradation under the most severe conditions in the test environment. The results demonstrated that by increasing the current density at the inflection point by reducing the cell pitch, the characteristics do not degrade at a current density of up to 2,000 A/cm^2, four times that at which conventional SiC trench gate MOSFETs have bipolar degradation.

5. Threading BPD Density Impact Evaluation

Next, we evaluated the dependence of SF expansion on the threading BPD density. We prepared substrates with different BPD densities from several vendors and formed epitaxial film on them to make experimental SBD-integrated MOSFETs. We used them to verify whether the same effect of bipolar degradation suppression could be achieved. We especially tested the selected chips that include threading BPDs by performing PL imaging measurements to evaluate surface distribution of threading BPD in the drift layer that is formed on the epitaxial substrate for the prototypes. The device structure was the same as that of device C, which did not experience bipolar degradation in Section 4. After the initial measurement, we applied a forward DC of 100 A/cm^2 for 10 minutes at 150°C and a pulse current of 2,000 A/cm^2 for 2 minutes at 175°C to the prototypes.

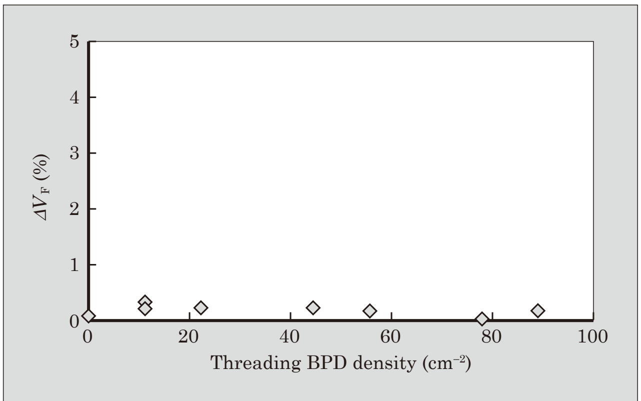

Fig.10 ΔV_F versus threading BPD density

Figure 10 shows ΔV_F versus threading BPD density contained in each chip. For all the evaluated devices, we confirmed that the amount of fluctuation was small compared with initial value before activation and that there was no degradation of the characteristics. The results demonstrate that integrating an SBD is effective in suppressing bipolar degradation, regardless of the density of the threading BPD.

6. Postscript

We conducted research on a structure that integrates an SBD in a MOSFET as a technology to suppress bipolar degradation caused by body diode activation. By using a trench SBD structure, the SBD can be integrated with the characteristics no less than that of the conventional SiC trench gate MOSFETs.

We estimated the current density at which bipolar degradation is suppressed from the inflection point indicated by the J-V characteristics of the body diode. Based on the evaluation, we showed that the narrower the cell pitch, the higher the suppression effect. Actual forward bias stress tests have demonstrated that no characteristic degradation occurs up to a current density of 2,000 A/cm^2, which is four times the current density at which bipolar degradation occurs in conventional SiC trench gate MOSFETs. We also confirmed that bipolar degradation can be stably suppressed regardless of the threading BPD density of the epitaxial substrate.

This research was conducted as a project of the joint research body Tsukuba Power-Electronics Constellations (TPEC). We would like to express our gratitude to Shinsuke Harada and Tadao Morimoto of the National Institute of Advanced Industrial Science and Technology (AIST) for their cooperation in prototyping, evaluation, and consultation.

References

(1) Agarwall, A. et al. "A New Degradation Mechanism in High-Voltage SiC Power MOSFETs". IEEE Electron Device Lett. 28 (2007) 587-589.

(2) Skowronski, M. et al. "Recombination-enhanced defect motion in forward-biased 4H-SiC p-n diodes". J. Appl. Phys. 92 (2002) 4699-4704.

(3) Konishi, K. et al. "Stacking fault expansion from basal plane dislocations converted into threading edge dislocations in 4H-SiC epilayers under high current stress" J. Appl. Phys. 114 (2013) 014504-1-0145045.

Supplemental Explanation

Explanation 1 Arm

p. 175, 188

In switching circuits such as inverters, the parts that are made up of switches and diodes are called arms. As shown in Fig. 1, the circuit that supplies the load with an electric current from the power source is the upper arm. The circuit that draws electric current from the load to the power source is the lower arm.

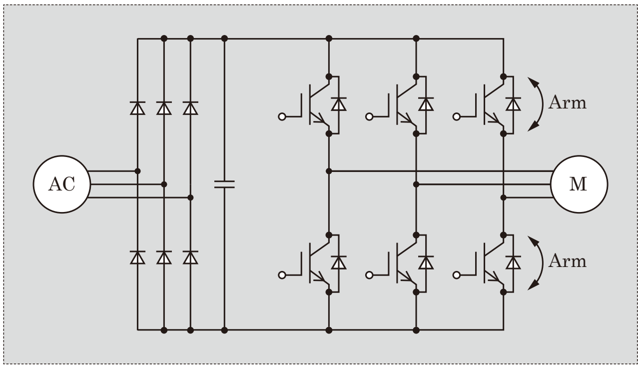

Fig.1 Switching circuit

Overseas Subsidiaries

＊Non-consolidated subsidiaries

Fuji Electric website
https://www.fujielectric.com/

America

Fuji Electric Corp. of America
Sales of electrical machinery and equipment, semiconductor devices, drive control equipment, and devices
URL https://americas.fujielectric.com/

Reliable Turbine Services LLC
Repair and maintenance of steam turbines, generators, and peripheral equipment
Tel +1-573-468-4045

Fuji SEMEC Inc.
Manufacture and sales of door opening and closing systems
Tel +1-450-641-4811

Asia

Fuji Electric Asia Pacific Pte. Ltd.
Sales of electrical distribution and control equipment, drive control equipment, and semiconductor devices
URL http://www.sg.fujielectric.com/

Fuji SMBE Pte. Ltd.
Manufacture, sales, and services relating to low-voltage power distribution board (switchgear, control equipment)
URL http://smbe.fujielectric.com/

Fuji Electric (Thailand) Co., Ltd.
Sales and engineering of electric substation equipment, control panels, and other electric equipment
URL http://www.th.fujielectric.com/en/

Fuji Electric Manufacturing (Thailand) Co., Ltd.
Manufacture, sales, engineering and service of low-voltage inverters, instrumentation and sensors, switchgear, gas insulated switchgear, PCS, UPS
Tel +66-2-5292178

Fuji Tusco Co., Ltd.
Manufacture and sales of Power Transformers, Distribution Transformers and Cast Resin Transformers
URL http://www.ftu.fujielectric.com/

Fuji Electric Vietnam Co.,Ltd. *
Sales of electrical distribution and control equipment and drive control equipment
URL http://www.vn.fujielectric.com/en/

Fuji Furukawa E&C (Vietnam) Co., Ltd. *
Engineering and construction of mechanics and electrical works
Tel +84-4-3755-5067

Fuji CAC Joint Stock Company
Provide the Solution for Electrical and Process Control System
URL http://fujicac.com/

PT. Fuji Electric Indonesia
Sales of inverters, servos, UPS, tools, and other component products
URL http://www.id.fujielectric.com/

P.T. Fuji Metec Semarang
Manufacture and sales of vending machines and their parts
URL http://www.fms.fujielectric.com/

Fuji Electric India Pvt. Ltd.
Sales of drive control equipment and semiconductor devices
URL http://www.fujielectric.co.in

Fuji Electric Consul Neowatt Private Limited
Development, manufacuture, engineering, sales and servicing of UPS, Stabilizers, Active Harmonic Filters and other component products
URL https://www.india.fujielectric.com/

Fuji Gemco Private Limited
Design, manufacture, sales, and engineering for drive control systems
Tel +91-129-2274831

Fuji Electric Philippines, Inc.
Manufacture of semiconductor devices
Tel +63-2-844-6183

Fuji Electric Sales Philippines Inc.
Sales of energy management systems, process automation systems, factory automation systems, power supply and facility systems, and power generation
URL https://www.ph.fujielectric.com/

Fuji Electric (Malaysia) Sdn. Bhd.
Manufacture of semiconductor devices
URL http://www.fujielectric.com.my/

Fuji Electric Sales Malaysia Sdn. Bhd.
Sales of energy management systems, process automation systems, factory automation systems, power supply and facility systems, and vending machines
URL https://www.my.fujielectric.com/

Fuji Furukawa E&C (Malaysia) Sdn. Bhd. *
Engineering and construction of mechanics and electrical works
Tel +60-3-4297-5322

Fuji Electric Taiwan Co., Ltd.
Sales of semiconductor devices, electrical distribution and control equipment, and drive control equipment
URL http://www.fujielectric.com.tw/

Fuji Electric Korea Co., Ltd.
Sales of power distribution and control equipment, drive control equipment, rotators, high-voltage inverters, electronic control panels, medium- and large-sized UPS, and measurement equipment
URL http://www.fujielectric.co.kr/

Fuji Electric Co.,Ltd. (Middle East Branch Office)
Promotion of electrical products for the electrical utilities and the industrial plants
Tel +973-17 564 569

Fuji Electric Co., Ltd. (Myanmar Branch Office)
Providing research, feasibility studies, Liaison services
Tel +95-1-8382714

Representative office of Fujielectric Co., Ltd. (Cambodia)
Providing research, feasibility studies, Liaison services
Tel +855-(0)23-964-070

■Equity-method Affiliates

Fuji Furukawa E&C (Thailand) Co., Ltd. *
Design and installation contracting for electric facilities construction
Tel +66-2-308-2703

Europe

Fuji Electric Europe GmbH
Sales of electrical/electronic machinery and components
URL https://www.fujielectric-europe.com/

Fuji Electric France S.A.S
Manufacture and sales of measurement and control devices
URL https://www.fujielectric.fr/en

Fuji N2telligence GmbH *
Sales and engineering of fuel cells and peripheral equipment
Tel +49 (0) 3841 758 4500

China

Fuji Electric (China) Co., Ltd.
Sales of locally manufactured or imported products in China, and export of locally manufactured products
URL http://www.fujielectric.com.cn/

Shanghai Electric Fuji Electric Power Technology (Wuxi) Co., Ltd.
Research and development for, design and manufacture of , and provision of consulting and services for electric drive products, equipment for industrial automation control systems, control facilities for wind power generation and photovoltaic power generation, uninterruptible power systems, and power electronics products
Tel +86-510-8815-9229

Wuxi Fuji Electric FA Co., Ltd.
Manufacture and sales of low/high-voltage inverters, temperature controllers, gas analyzers, and UPS
Tel +86-510-8815-2088

Fuji Electric (Changshu) Co., Ltd.
Manufacture and sales of electromagnetic contactors and thermal relays
URL http://www.csfe.com.cn/

Fuji Electric (Zhuhai) Co., Ltd.
Manufacture and sales of industrial electric heating devices
URL http://www.fujielectric.com.cn/fez/

Fuji Electric (Shenzhen) Co., Ltd.
Manufacture and sales of photoconductors, semiconductor devices and currency handling equipment
URL http://www.szfujielectric.com.cn/

Fuji Electric Dalian Co., Ltd.
Manufacture of low-voltage circuit breakers
Tel +86-411-8762-2000

Fuji Electric Motor (Dalian) Co., Ltd.
Manufacture of industrial motors
Tel +86-411-8763-6555

Dalian Fuji Bingshan Vending Machine Co., Ltd.
Development, manufacture, sales, servicing, overhauling, and installation of vending machines, and related consulting
Tel +86-411-8754-5798

Dalian Fuji Bingshan Control Systems Co., Ltd.
Energy management systems, distribution systems, and related system engineering
Tel +86-411-8653-6010

Fuji Electric (Hangzhou) Software Co., Ltd.
Development of vending machine-related control software and development of management software
URL http://www.fujielectric.com.cn/fhs/

Fuji Electric FA (Asia) Co., Ltd.
Sales of electrical distribution and control equipment
Tel +852-2311-8282

Fuji Electric Hong Kong Co., Ltd.
Sales of semiconductor devices and photoconductors
URL http://www.hk.fujielectric.com/en/

Hoei Hong Kong Co., Ltd.
Sales of electrical/electronic components
URL http://www.hoei.com.hk/

FUJI ELECTRIC REVIEW is made of environmentally friendly paper certified by the Forest Stewardship Council® (FSC) and printed with vegetable ink.

MIX Paper from responsible sources FSC® C017911

VEGETABLE OIL INK